TITLE PAGE

In vivo intrabursal administration of bioactive lipid sphingosine-1-phosphate enhances vascular integrity in a rat model of ovarian hyperstimulation syndrome (OHSS)

Running title: S1P restores the vascular integrity in OHSS.

Authors:

Mariana Di Pietro[1, ‡], Natalia Pascuali[1, ‡], Leopoldina Scotti[1], Griselda Irusta[1], Diana Bas[1], María May[3], Marta Tesone[1, 2], Dalhia Abramovich[1] and Fernanda Parborell[1]

[1] Instituto de Biología y Medicina Experimental (IByME) – CONICET, Buenos Aires, Argentina.

[2] Departamento de Química Biológica, Facultad de Ciencias Exactas y Naturales, Universidad de Buenos Aires, Buenos Aires, Argentina.

[3] Instituto de Investigaciones Farmacológicas (ININFA-UBA-CONICET), Facultad de Farmacia y Bioquímica, Universidad de Buenos Aires, Buenos Aires, Argentina.

‡Contributed equally

***Correspondence address:** e-mail: fparborell@gmail.com

ABSTRACT

Study question: Can the bioactive lipid sphingosine-1 phosphate (S1P) act as an endothelial barrier-enhancing molecule and, in turn, restore the vascular integrity and homeostasis in a rat model of ovarian hyperstimulation syndrome (OHSS).

Study answer: *In vivo* administration of S1P may prevent the early onset of OHSS and decrease its severity.

What is known already: Although advances in the prediction and treatment of OHSS have been made, complete prevention has not been possible yet. S1P in follicular fluid from women at risk of developing OHSS are lower in comparison from women who are not at such risk and administration of S1P in an OHSS rat model decreases ovarian capillary permeability.

Study design, size, duration: We used an animal model that develops OHSS in immature Sprague-Dawley rats. The rats were randomly divided into three groups: the control group, which was injected with 10 IU of pregnant mare's serum gonadotropin (PMSG), and 10 IU of human chorionic gonadotropin (hCG) 48 h later; the OHSS group, which was injected with excessive doses of PMSG (50 IU/day) for 4 consecutive days, followed by hCG; and the OHSS + S1P group, which was injected with the same doses of PMSG and hCG as the OHSS group and then treated with 5 µl S1P (1 mM) under the bursa of both ovaries, whereas the other groups of animals received the S1P vehicle.

Participants/materials, setting, methods: Rats were killed by decapitation 48 h after the hCG injection for ovary, endometrium and blood collection. The ovaries were weighed and then used for subsequent assays, while the serum was used for hormone

assays. One of the ovaries from each rat (n=6) was used for Western immunoblot and the other for immunohistochemical analysis. Statistical comparisons between groups were carried out.

Main results and the role of chance: S1P administration reduced the ovarian weight ($p<0.05$), and decreased the concentration of serum progesterone in the OHSS group compared to the OHSS group without treatment ($p<0.001$). The percentage of antral follicles in the OHSS group was lower than that in the control group. S1P increased the percentage of antral follicles ($p<0.05$) and decreased the percentage of corpora lutea ($p< 0.01$) and cystic structures in the OHSS group ($p<0.05$)**.** S1P had no effect on the expression levels of the enzymes 3β-hydroxysteroid dehydrogenase (3βHSD) or cholesterol side-chain cleavage enzyme (P450scc), but reduced the levels of steroidogenic acute regulatory protein (StAR) in OHSS rat ovaries. ($p<0.05$). S1P decreased the endothelial ($p<0.05$) and periendothelial ($p<0.01$) cell area in OHSS rat ovaries. S1P restored the levels of N-cadherin and VE-cadherin proteins to control values. Furthermore, S1P enhanced the levels of claudin-5, occludin ($p<0.05$) and sphingosine-1-phosphate receptor 1 (S1PR1) in OHSS ($p<0.01$). In addition, no histological differences were found in endometrium between OHSS and S1P-treated OHSS animals.

Limitations, reasons for caution: The results of this study were generated from an *in vivo* OHSS experimental model, which has been used by several authors and our group due to the similarity between the rat and human angiogenic systems. Further studies in patients will be needed to evaluate the effects of S1P in the pathogenesis of OHSS.

Wider implications of the findings: These findings concern the pathophysiological importance of S1P in OHSS. More studies on the regulation of endothelial cell barrier

function by S1P in reproductive pathological processes and its therapeutic application are required.

Large scale data: N/A.

Study funding and competing interest(s): This work was supported by grants from ANPCyT (PICT 2012-897), CONICET (PIP 5471), Roemmers and Baron Foundations, Argentina. The authors declare no conflicts of interest.

Key words: angiogenesis, ovary, OHSS, sphingolipids, vascular integrity

INTRODUCTION

Ovarian hyperstimulation syndrome (OHSS) is one the most serious iatrogenic complications of follicular growth and maturation induced by ovulation induction. It is characterized by increased vascular leakage and ovarian enlargement, which cause fast third space fluid shifts from the intravascular compartment (Delvigne and Rozenberg 2002, Aboulghar and Mansour 2003). These shifts are caused by increased vascular permeability in response to stimulation with human chorionic gonadotropin (hCG) (Gomez *et al.,* 2010). The patho-physiology of OHSS is not completely understood, and no specific therapy or prevention is available yet (Rizk and Aboulghar 1991, Fiedler and Ezcurra 2012). It is recognized that this syndrome is triggered by hCG (Gomez *et al.,* 2010) and that the predominant link between hCG and OHSS is the production of angiogenic factors. Several pro-angiogenic factors, including members of the Vascular Endothelial Growth Factor A (VEGFA) family, angiopoietins (ANGPTs), transforming growth factors (TGFs), platelet-derived growth factors (PDGFs) and sphingosine-1 phosphate (S1P), have been identified (Neufeld *et al.,* 1999, Fiedler and Augustin 2006, Armulik *et al.,* 2005, Carmeliet 2000, Hanahan and Folkman 1996, Neufeld *et al.,* 1999, Otrock *et al.,* 2007, Allende and Proia 2002). One of the main functions of

PDGFs and S1P, unlike VEGFA and ANGPTs, is the stabilization of newly developed capillaries (Hoch and Soriano 2003, Allende *et al.,* 2003, Xiong and Hla 2014).

Previously, we have evaluated the involvement of ANGPTs and PDGFs in this syndrome and we have observed that PDGF-B and -D protein levels decrease in ovaries from an OHSS rat model, while ANGPT2 and PDGFR-β levels remain constant (Scotti *et al.,* 2013). Furthermore, we have shown that ANGPT1 concentration is higher in follicular fluids (FF) from women at risk of developing OHSS than in FF from control patients, whilst the levels of the soluble form of the receptor Tie-2 (sTie-2) remain unchanged. Additionally, inhibition of ANGPT1 in FF from OHSS patients by the use of a neutralizing antibody decreases endothelial cell migration in comparison with untreated FF from OHSS women (Scotti *et al.,* 2013). Recently, we have observed that the levels of sphingolipid S1P in FF from women at risk of developing OHSS are lower in comparison with FF from women who are not at such risk, while the addition of S1P to the FF restores vascular integrity in an endothelial cell culture (Scotti L. *et al.,* 2016). Additionally, we have shown in the same study that *in vivo* intrabursal administration of S1P in an OHSS rat model decreased ovarian capillary permeability and ovarian expression of VEGF and its receptor KDR. All these findings suggest that the ANGPT, PDGF and S1P systems could be partly responsible for the characteristic increase in ovarian vascular permeability in OHSS.

S1P is derived from sphingosine phosphorylation by sphingosine kinase (Spiegel and Milstien 2003) and its degradation can be either mediated by S1P lyase (SPL) or by S1P phosphatases (Ogawa *et al.,* 2003, Le Stunff *et al.,* 2002). Not only is S1P secreted by activated platelets, but also erythrocytes, mononuclear cells, neutrophils and mastocytes can release this lipid mediator (Yatomi *et al.,* 1995, Yang *et al.,* 1999). S1P binds to specific cell surface receptors (S1PRs), which comprise a G-protein-coupled receptor family including subtypes S1PR1, S1P2, S1P3, S1P4 and S1P5. S1P is present in blood and plasma

and delivered to its receptors by high-density lipoprotein (HDL)-associated apoliprotein M (Singleton *et al.,* 2006). S1P is a pleiotropic sphingolipid capable of modulating the functions of various cell types (Xiong and Hla 2014). In particular, it regulates several physiological responses in vascular cells (Obinata and Hla 2012) and promotes endothelial cell spreading, vascular maturation/stabilization, and barrier function (Xiong and Hla 2014). The alteration of vascular barrier integrity causes serious consequences such as inflammation, edema, haemorrhage and ischemia. S1P has been proposed as a barrier-enhancing molecule and as a potential candidate for novel and specific therapies for endothelial dysfunction (Sanchez *et al.,* 2003, Jung *et al.,* 2012, Gaengel *et al.,* 2012b). In this regard, Dudek *et al.* (2004) and Liu *et al.* (2009) have shown that S1P administration in animal models with acute lung injury decreases vascular hyperpermeability by the enhancement of endothelial junctional integrity (Dudek *et al.,* 2004, Liu *et al.,* 2009). Furthermore, Curry *et al.* (2012) have previously shown that exogenous S1P attenuates acute microvascular permeability via receptor S1PR1 and stabilizes the endothelium in rats (Curry *et al.,* 2012).

The expression of S1PRs (S1PR1, S1P2 and S1P3) has been shown in female reproductive tissues and granulosa cells (Wang *et al.,* 2014, Kon *et al.,* 1999, Risau 1997). Also, several authors have previously documented the role of S1P in reproduction. Roth and Hansen (2004) have demonstrated that S1P may improve fertility when developmental competence of the oocytes is compromised (Roth and Hansen 2004). Other researchers have proposed S1P as a potential candidate for fertility preservation of female cancer patients (Li *et al.,* 2014, Meng *et al.,* 2014, Morita and Tilly 2000).

However, there are no studies on the effect of *in vivo* intrabursal S1P administration on ovarian morphology or vascular development and integrity in a rat model of OHSS. Therefore, the main purpose of this study was to evaluate the effects of local S1P

administration on ovarian weight, follicular and luteal development, formation of cystic structures, steroidogenesis, endothelial and periendothelial area (pericytes and smooth muscle cells), and on adherens and tight junction protein expression in ovaries from an OHSS rat model stimulated by equine chorionic gonadotropin (eCG), and hCG. In this model, we assessed the effect of S1P administration on S1PR1 protein expression in ovaries. Additionally, in this model we evaluated the effect of S1P on uterine morphology.

MATERIALS AND METHODS

Ethical approval

All procedures were approved by the ethics committee of the IByME (CE-018-2/2012) and conducted according to the guide for the care and use of laboratory animals of the National Institute of Health (USA).

Animal model and experimental design

Rats were housed and cared at the Instituto de Biología y Medicina Experimental (IByME), Buenos Aires, Argentina. Immature female Sprague-Dawley rats (21–23 days old) from our colony (n=6/group for each treatment) were allowed food and water *ad libitum* and kept at room temperature (21–23°C) on a 12L:12D cycle. We used an animal model that develops OHSS in immature Sprague-Dawley rats (21–23 days, 60–80 g), as described by Kitajima et al. (2004, 2006). The control group (n=6) was injected with 10 IU eCG and with 10 IU hCG 48 h later. The OHSS group (n=6) was injected with 50 IU eCG for four consecutive days, followed by 25 IU of hCG. The OHSS + S1P group (n=6) received the same doses of eCG and hCG as the OHSS group and was also treated with S1P. To administrate S1P on the day of hCG injection, the animals were anesthetized with ketamine HCl (70 mg/Kg; Holliday-Scott S.A., Buenos Aires, Argentina) and xylazine (5 mg/Kg; König Laboratories, Buenos Aires, Argentina) and the ovaries were exteriorized through an incision made in the dorsal

lumbar region. The OHSS+S1P group received 5 µl S1P (1 mM) (Sigma Aldrich (St. Louis, MO, USA) under the bursa of both ovaries (Hernandez *et al.,* 2009), whereas the other groups received the S1P vehicle (0.8% Tween-80; 2.5% ETOH; 5% polyethylene glycol (PEG).

Rats were killed by decapitation 48 h after the hCG injection for ovary and blood collection. The ovaries were removed and cleaned of adhering tissue in culture medium, weighed, and used for subsequent assays. The serum was used for hormone assays. One ovary from each rat (n=6) was used for Western blotting and the other for immunohistochemical analysis.

Steroid hormone assay

Serum steroid concentrations were measured by radioimmunoassay (RIA) (n=6 rats/group) (Irusta *et al.,* 2003, Irusta *et al.,* 2007). Progesterone (P_4) was measured by using specific antibodies supplied by Dr. G.D. Niswender (Animal Reproduction and Biotechnology Laboratory, Colorado State University, Fort Collins, CO, USA). Under these conditions, the intra- and inter-assay variations for P_4 were 8.0% and 14.2% respectively. The values are expressed per ml of serum.

Ovarian and endometrium morphology

Ovaries and uterine horns were extracted from the different experimental groups and immediately fixed in Bouin solution for 12 h. Histological sections were made for haematoxylin-eosin (H&E) staining. Ovarian sections (5 µm) were mounted at 50-µm intervals onto microscope slides to prevent counting the same structure twice, according to the method described by Woodruff *et al.* (Woodruff *et al.,* 1988). Preantral follicles, antral follicles, atretic follicles, corpora lutea (CL) and cystic structures were counted in six ovarian sections from each ovary (n=6 ovaries/group) and expressed as structure percentage per

ovary. The total number of ovarian structures was defined as 100%. Cysts were defined as structures with presence of oocytes surrounded by luteal cells, remaining granulosa cells and red blood cells (Scotti *et al.,* 2014c). A set of uterine sections was stained with H&E and examined microscopically by an experienced gynecologic pathologist, who was blinded to the group assignment.

Histochemistry and immunohistochemistry in luteal tissues

Tissue sections were deparaffinized in xylene and rehydrated by graduated ethanol washes. Endogenous peroxidase activity was blocked with hydrogen peroxide in PBS and nonspecific binding was blocked with 2% bovine serum albumin (BSA) overnight at 4ºC. Sections were incubated with biotinylated lectin BS-1 (from *Bandeiraea simplicifolia*, 20 μg/ml, Vector Laboratories, Burlingame, CA, USA) or α-SMA (smooth muscle actin) 1/250 (ab18147 Abcam, Cambridge, USA) overnight at 4ºC. Lectin BS-1 has demonstrated to be a constitutive endothelial cell marker staining endothelial cells at the different developmental stages of CL with similar intensity (Augustin *et al.,* 1995, Redmer *et al.,* 2001, Cherry *et al.,* 2008). After washing, slides were incubated with biotinylated anti-mouse IgG (except in the case of lectin BS-1) and afterwards with avidin-biotinylated horseradish peroxidase Complex (Vectastain ABC system from Vector Laboratories) for 30 min. Protein expression was visualized with diaminobenzidine (DAB) staining. After stopping the reaction with distilled water, slides were stained with haematoxylin, dehydrated and mounted (Canada Balsam Synthetic, Biopack, Argentina). Negative controls were obtained in absence of primary antibody.

The images were digitized with a camera (Nikon, Melville, NY, USA) mounted on a conventional light microscope (Nikon), using a magnification of 40X. Three sections per ovary were analysed (six ovaries/group) and at least four corpora lutea were photographed

per section. Images were converted to TIFF format for analysis and processed using Image Pro-Plus 3.0 ® (Media Cybernetics, Silver Spring, MA, USA). Endothelial and peri-endothelial cell areas were determined by thresholding each lectin BS-1- or α-SMA-positive stained areas, which were then normalised to the total area of the analysed corpus luteum.

Western blot

Ovaries were removed, placed on ice and resuspended in five volumes of lysis buffer (20 mM Tris-HCl pH 8, 137 mM NaCl, 1% Nonidet P-40 and 10% glycerol) supplemented with protease inhibitors (0.5 mM PMSF, 0.025 mM N-CBZ-$_L$-phenylalanine chloromethyl ketone, 0.025 mM N-p-tosyl-lysine chloromethyl ketone and 0.025 mM $_L$-1-tosylamide-2-phenyl-ethylchloromethyl ketone) and homogenized with an Ultra-Turrax homogenizer (IKA Werk, Breisgau, Germany). Samples were centrifuged at 4ºC for 10 min at 10,000 x g and the resulting pellets were discarded. Protein concentration in the supernatant was measured by the Bradford assay. After boiling for 5 min, 40 µg of protein was applied to a 12% SDS-polyacrylamide gel and electrophoresis was performed at 25 mA for 1.5 h. The resolved proteins were transferred onto nitrocellulose membranes for 2 h. The blot was then incubated in blocking buffer (5% nonfat milk, 0.05% tween-20 in 20 mM TBS pH 8.0) for 1 h at room temperature and incubated overnight at 4°C with appropriate primary antibodies: StAR 1/1000 was donated by Dr. D. M. Stocco (Texas Tech University Health Sciences Center); P450scc 1/2000 was donated by Dr. Anita Payne (Stanford University Medical Center, Stanford, CA, USA); S1PR1 (ab125074) was from Abcam (Cambridge, USA), 3βHSD 1/1000 (sc-30820), VE-cadherin 1/100 (sc-9989), N-cadherin 1/250 (sc-7939) and Nectin-2 1/200 (sc-373715) were from Santa Cruz Biotechnology, Inc. (Santa Cruz, CA, USA); and Claudin-5 1/1000 (35-2500), occludin: 1/1000 (71–1500) were from Invitrogen Corp. (Carlsbad, CA, USA), β-actin 1/10000 (4967) and GAPDH 1/10000 (14C10) were from Cell

Signaling Technology, INC (Baverly, MA, USA). The blot was then incubated with anti-mouse or anti-rabbit secondary antibodies conjugated with horseradish peroxidase (1:1000) and signal was detected by chemiluminescence. The protein levels were analysed by densitometry using Scion Image for Windows (Scion Corporation, Worman's Mill, CT, USA). Optical density data are expressed as arbitrary units ± SEM. The density in each band was normalised to the density of the β-actin or GAPDH band, which were used as an internal control.

Data analysis

The results are expressed as the mean ± SEM and the significant differences between groups were determined using analysis of variance (ANOVA), followed by Tukey's test. *P* values <0.05 were considered statistically significant. All samples were tested for normality before ANOVA. Data were statistically analysed using Prism v5.0.

RESULTS

Effect of S1P on ovarian weight and progesterone (P_4) concentration in the rat model of OHSS.

The effects of S1P on ovarian weight and P_4 serum concentration are summarized in Table I. The ovarian weight in the OHSS group was higher compared to the control group ($p<0.001$). S1P administration reduced the ovarian weight observed in the OHSS group without treatment ($p<0.05$). Serum P4 concentration in the OHSS group was higher than that in the control group ($p<0.001$). S1P treatment decreased the concentration of serum P_4 compared with the untreated OHSS group ($p<0.001$).

Effect of S1P on ovarian morphology and steroidogenic enzyme expression in the rat model of OHSS.

The percentage of antral follicles in the OHSS group was lower than that in the control group. In the OHSS+S1P group, the percentage of antral follicles increased compared to the OHSS group without treatment ($p<0.05$) (Fig. 1B). However, no significant differences were observed in the percentage of preantral or atretic follicles among the three experimental groups (Fig. 1A and C). The percentage of CL in the OHSS group increased significantly compared with that in the control group ($p<0.05$) (Fig. 1D). Local administration of S1P reduced the percentage of CL ($p<0.01$) and cystic structures in comparison with the untreated OHSS group ($p<0.05$) (Fig. 1D and E).

To evaluate the effect of S1P on steroidogenesis in the OHSS rat model, we studied the expression of 3βHSD, P450scc and StAR. The levels of these enzymes in the OHSS group were higher than those in the control group (3βHSD: $p<0.05$; P450scc: $p<0.01$; StAR: $p<0.05$) (Fig. 2). S1P administration had no effect on the expression levels of 3βHSD or P450scc in OHSS rat ovaries (Fig. 2A and B), but decreased StAR levels compared to the untreated OHSS group ($p<0.05$) (Fig. 2C).

Effect of S1P on luteal vascular development in the rat model of OHSS.

To evaluate whether S1P treatment causes changes on endothelial cells present in corpora lutea, we stained ovarian sections for lectin BS-1. The endothelial cell area in the OHSS group was higher than that in the control group ($p<0.001$), while S1P administration decreased the endothelial cell area compared to OHSS group ($p<0.001$) (Fig. 3A).

Also, we evaluated luteal vascular stability in ovarian sections immunostained with α-SMA antibody. The periendothelial cell area in the OHSS group was lower than that in

the control group ($p<0.001$), while S1P increased the periendothelial cell area compared to the OHSS group without treatment ($p<0.05$) (Fig. 3B).

Effect of S1P on the expression of endothelial cell-to-cell junction proteins in the rat model of OHSS.

The levels of N-cadherin and VE-cadherin were lower in the OHSS group than in the control group ($p<0.05$). Local administration of S1P restored the levels of these proteins to control values (Fig. 4 A and B).

The levels of the tight junction proteins claudin-5, occludin and Nectin-2 were lower in the OHSS group in comparison with the control group (claudin-5: $p<0.01$; occludin: $p<0.001$; Nectin-2: $p<0.05$). S1P treatment increased the levels of claudin-5 and occludin compared to those in the OHSS group ($p<0.05$), whereas the levels of Nectin-2 remained unchanged (Fig. 4 C, D and E).

Effect of S1P on the expression of S1PR1 in the rat model of OHSS.

The ovarian levels of S1PR1 in the OHSS group were similar to those in the control group. In the OHSS+S1P group, the levels of S1PR1 increased compared to those of the OHSS group ($p<0.01$) (Fig. 5).

Effect of S1P on uterine morphology in the rat model of OHSS

The endometrium from the control group showed a few residual glands surrounded by an atrophic, somewhat fibrotic stroma. The epithelium was low cuboidal or columnar with almost no mitotic figures (Fig. 6).

The endometrium of the OHSS and S1P-treated OHSS groups showed a columnar surface epithelium with slight pseudostratification and small, round and regular glands. In addition,

endometrial stroma showed no edema but occasional mitotic figures, and small and regularly distributed blood vessels. No histological differences were found in endometrium between OHSS and S1P-treated OHSS animals.

DISCUSSION

The main clinical characteristics of OHSS are ovarian enlargement, with luteal and haemorrhagic cysts, and increased vascular permeability (Golan *et al.,* 1989, Gomez *et al.,* 2010). Previously, we and other authors have demonstrated that VEGF, ANGPTs, PDGFs could be mediators in the development of OHSS (Artini *et al.,* 1998, Pellicer *et al.,* 1999, Scotti *et al.,* 2014d, Scotti *et al.,* 2014b, Scotti *et al.,* 2013). Recently, we have shown that S1P levels are lower in FF from patients at risk of OHSS and that treatment with S1P may decrease vascular permeability in these patients (Scotti L. *et al.,* 2016).

In the current study, we present evidence for the first time that S1P intrabursal administration *in vivo* affects ovarian weight, follicular and luteal development, formation of cystic structures and steroidogenesis in ovaries from a rat OHSS model. Additionally, we observed that local administration of this sphingolipid causes a decrease in the endothelial area, an increase in both the peri-endothelial area and N-cadherin, VE-cadherin, claudin-5 and S1PR1 receptor protein levels in the ovaries of the above-mentioned model.

In humans, OHSS generates the formation of multiple CL and the increase of VEGF levels (Navot *et al.,* 1992). Our study is the first to demonstrate that administration of S1P *in vivo* in ovaries from OHSS rats affects luteal development, delays folliculogenesis and leads to a lower percentage of CL. These results suggest that, as S1P decreases the presence of CL, which secrete several angiogenic factors that in turn favour an altered angiogenesis, this lipid metabolite is also likely to ameliorate the vascular permeability observed in OHSS. The decrease in CL and cystic structures in the S1P-treated ovaries is consistent with the decrease

in serum P_4 and ovarian weight observed. It is known that the transport of cholesterol from the cytoplasm to the inner mitochondrial membrane, mediated by the StAR protein, is the limiting step in progesterone (P_4) synthesis. Therefore, the diminished expression of StAR, as demonstrated by Western blot, could be partly responsible for the decrease in serum P_4 in the S1P-treated OHSS rats. These results are consistent with those obtained by other authors such as Budnik *et al.* (2005), who have shown that S1P suppresses P_4 synthesis in luteal cells and Leydig tumour cells stimulated with luteotropic hormone or a cAMP analog (Budnik and Brunswig-Spickenheier 2005). It is worth noting that S1P did not affect ovarian expression of P450scc or 3βHSD, which are critical for biosynthesis of steroid hormones.

CL are highly vascularized structures, whose vascular development exceeds that of most tumours (Reynolds *et al.,* 2000). In this study, the *in vivo* administration of S1P may have altered the formation and function of CL by preventing angiogenesis in OHSS. The decrease in luteal endothelial cell area after S1P administration suggests that the sphingolipid caused a decrease in the number of endothelial cells, and thus a decrease in the luteal microvasculature that likely contributed to the decrease in serum P_4 concentrations. Pericyte coverage induces vessel maturation by resolving angiogenic signals and reducing endothelial proliferation. Thus, the recruitment of peri-endothelial cells and the deposition of basal membranes represent crucial steps to achieve vascular maturation (Potente *et al.,* 2011). In our study, S1P was able to increase the recruitment of pericytes and smooth muscle cells, enhancing pericyte-endothelium interaction and, in turn, improving luteal vessel stability in OHSS. It is worth noting that the breakdown of the S1P signalling system results in pathological hyperpermeability such as acute lung injury, anaphylaxis and inflammation (Peng *et al.,* 2004, Olivera *et al.,* 2003).

Controlled dynamic changes in the localization and expression of adhesion molecules are essential in the ovary (Groten *et al.,* 2006, Rodewald *et al.,* 2007). This includes regulation

of adherens and tight junctions (AJ and TJ), which are key components of intercellular junctions (Dejana 2004, Schneeberger and Lynch 2004). An increase in endothelial permeability is generally accompanied by reorganization of junctional proteins, inducing a transient opening of the endothelial junctions and an increment in vascular permeability (Bazzoni and Dejana 2004, Dejana 2004, Walz *et al.,* 2005). TJ proteins, which are composed of at least three different families of transmembrane proteins (claudins, occludins and junction adhesion molecules), represent a barrier to molecule diffusion from the vessel lumen to the tissue parenchyma (Groten *et al.,* 2006), whereas AJ proteins involve transmembrane proteins belonging to the cadherin family. Thus, we propose that TJ and AJ proteins are downstream targets of S1P in vascular cells of ovaries from animals with OHSS. Since VE-cadherin is the main structural protein of AJ in endothelial cells (Mehta *et al.,* 2005), we decided to study the levels of this protein in the OHSS rat model. We and other authors showed the importance of this cadherin in the development of OHSS (Villasante *et al.,* 2007, Scotti *et al.,* 2014a). We have previously observed that VE-cadherin levels decrease significantly in endothelial cells incubated with FF from OHSS patients compared to control patients. In the present study, we observed that S1P is able to restore the levels of VE-cadherin, contributing to the sealing of the intercellular space and reducing vascular permeability in the ovary. These results are consistent with recently obtained studies in our laboratory, as we found that S1P addition increased VE-cadherin expression and reduced VEGF expression in endothelial cells compared to FF from patients at risk of OHSS without the sphingolipid (Scotti L. *et al.,* 2016). Regarding this point, Gaengel *et al.* (2012) have studied the communication between the VEGF and S1P systems and demonstrated that when co-stimulating human umbilical vein endothelial cells (HUVEC) with VEGF and S1P, VE-cadherin remained stable in endothelial junctions and was insensitive to the internalization induced by VEGF (Gaengel et al., 2012). Additionally, Lee *et al.* (1999) have demonstrated

that S1P increases the VE-cadherin and β-catenin levels and, in turn, enhances AJ assembly in confluent HUVEC (Lee *et al.,* 1999). Furthermore, Krump-Konvalinkova *et al.* (2005) have shown that S1PR1 silencing decreases the expression of platelet-endothelial cell adhesion molecule-1 (PECAM) and VE-cadherin human endothelial cell lines (Krump-Konvalinkova *et al.,* 2005).

Besides VE-cadherin, N-cadherin also regulates vascular stability since it mediates pericyte adhesion to endothelial cells, enhancing vessel maturation and stabilization (Volk and Geiger 1984, Tillet *et al.,* 2005). In the present study, S1P restored the levels of N-cadherin suggesting that, in OHSS, S1P improves the endothelial-pericyte interaction mediated by this cadherin, contributing to vessel maturation and endothelial barrier integrity. This supports previous data from our laboratory, where we have shown that S1P addition increased N-cadherin levels in endothelial cells compared to FF from patients at risk of OHSS without the sphingolipid (Scotti L. *et al.,* 2016). Furthermore, Paik *et al.* (2004) have shown that the inhibition of N-cadherin affects vascular stabilization *in vitro* and *in vivo*, suggesting a specific involvement of S1P in N-cadherin-induced pericyte attachment (Paik *et al.,* 2004).

The nectin system has been described as a novel modulator of AJ and TJ, and provides the first scaffold for the formation of these junctions (Niessen 2007). Based on this information, we analysed the expression in the rat OHSS model of claudin-5 and occludin (TJ proteins), and also of nectin-2, the only member of the nectin system that is expressed in the endothelium of CL (Herr *et al.,* 2015). S1P was able to restore the decreased levels of claudin-5, occludin and nectin 2, contributing to the formation of TJ and ovarian vascular stability. Taking together these results suggests that S1P upregulates VE-cadherin, N-cadherin, claudin-5 and occludin and consequently reduces vascular permeability in OHSS. Accordingly, S1P improves the assembly of AJ and assists in the formation of TJ.

Moreover, S1P is able to enhance endothelial maturation through its receptor, S1PR1, by promoting Rac1 activation and AJ assembly (Garcia *et al.,* 2001). Thus, we evaluated S1PR1 expression in the OHSS model. S1P was able to upregulate the expression of its own receptor, enhancing vascular integrity and, in turn, avoiding the aberrant angiogenic responses observed in OHSS. The precise mechanism by which the sphingolipid increases expression of its own receptor is currently unknown. These findings are in line with the observations by Gaengel *et al*. (2003), who demonstrated that S1PR1 signalling inhibits endothelial hyper-sprouting through stabilization of VE-cadherin and through inhibition of VEGFR2 phosphorylation (Gaengel *et al.,* 2012a).

We decided to evaluate possible side-effects of S1P treatment in other vascularized organs, such as the uterus. We did not observe any change in endometrial morphology after S1P treatment in the OHSS model.

In summary, our study shows that local S1P administration decreases the percentage of CL and cystic structures, serum P_4 concentrations, endothelial cell area, and StAR protein expression in ovaries from OHSS rats, and increases the percentage of antral follicles, peri-endothelial area, and S1PR1, AJ and TJ protein levels in OHSS rats.

Therefore, local administration of S1P decreased the vascular permeability and angiogenesis in the OHSS group. These effects would be directly mediated by the decrease in the percentage of the CL and in blood vessel development, and by the increase in vascular stability in the CL. Our findings would indicate for the first time that S1P acts in the rat OHSS model as an endothelial barrier-enhancing factor, restoring the vascular integrity and homeostasis in OHSS. S1P administration may therefore prevent the early onset of OHSS and decrease its severity. More studies on the regulation of endothelial cell barrier function by the bioactive lipid S1P in reproductive pathological processes and its therapeutic application are required.

Acknowledgements

We thank ANPCyT (PICT 2012-897), CONICET (PIP 5471), Roemmers Foundation and René Barón Foundation, Argentina, for supporting the study.

Authors' Roles

MD and NP performed the experiments and contributed to data analysis and interpretation.

LS discussed the results and helped draft the manuscript.

DB, GI and MT contributed to data interpretation and discussed the results.

DA analysed and discussed the results, and helped draft the manuscript.

MM performed the assessment of uterine morphology.

FP conceived the concept, designed the experiments, supervised the study and wrote the manuscript.

All the authors read and approved the final manuscript.

Funding

This study was supported by grants ANPCyT (PICT 2012-897), CONICET (PIP 5471), and Roemmers and Baron Foundations, Argentina.

Conflict of interest

The authors declare no potential conflicts of interest with respect to the research, authorship, and/or publication of this article.

475 **REFERENCES**

476

477 Aboulghar MA, Mansour RT. Ovarian hyperstimulation syndrome: classifications and
478 critical analysis of preventive measures. *Hum.Reprod.Update.*2003 **9**, 275-289.

479 Allende ML, Proia RL. Sphingosine-1-phosphate receptors and the development of the
480 vascular system. *Biochim.Biophys.Acta*2002 **1582**, 222-227.

481 Allende ML, Yamashita T, Proia RL. G-protein-coupled receptor S1P1 acts within
482 endothelial cells to regulate vascular maturation. *Blood*2003 **102**, 3665-3667.

483 Armulik A, Abramsson A, Betsholtz C. Endothelial/pericyte interactions. *Circ.Res.*2005
484 **97**, 512-523.

485 Artini PG, Monti M, Fasciani A, Tartaglia ML, D'Ambrogio G, Genazzani AR.
486 Correlation between the amount of follicle-stimulating hormone administered and
487 plasma and follicular fluid vascular endothelial growth factor concentrations in women
488 undergoing in vitro fertilization. *Gynecol.Endocrinol.*1998 **12**, 243-247.

489 Augustin HG, Braun K, Telemenakis I, Modlich U, Kuhn W. Ovarian angiogenesis.
490 Phenotypic characterization of endothelial cells in a physiological model of blood vessel
491 growth and regression. *Am.J.Pathol.*1995 **147**, 339-351.

492 Bazzoni G, Dejana E. Endothelial cell-to-cell junctions: molecular organization and role
493 in vascular homeostasis. *Physiol Rev.*2004 **84**, 869-901.

494 Budnik LT, Brunswig-Spickenheier B. Differential effects of lysolipids on steroid
495 synthesis in cells expressing endogenous LPA2 receptor. *J.Lipid Res.*2005 **46**, 930-941.

496 Carmeliet P. Fibroblast growth factor-1 stimulates branching and survival of myocardial
497 arteries: a goal for therapeutic angiogenesis? *Circ.Res.*2000 **87**, 176-178.

498 Cherry JA, Hou X, Rueda BR, Davis JS, Townson DH. Microvascular endothelial cells
499 of the bovine corpus luteum: a comparative examination of the estrous cycle and
500 pregnancy. *J.Reprod.Dev.*2008 **54**, 183-191.

501 Curry FE, Clark JF, Adamson RH. Erythrocyte-derived sphingosine-1-phosphate
502 stabilizes basal hydraulic conductivity and solute permeability in rat microvessels.
503 *Am.J.Physiol Heart Circ.Physiol*2012 **303**, H825-H834.

504 Dejana E. Endothelial cell-cell junctions: happy together. *Nat.Rev.Mol.Cell Biol*2004 **5**,
505 261-270.

506 Delvigne A, Rozenberg S. Epidemiology and prevention of ovarian hyperstimulation
507 syndrome (OHSS): a review. *Hum.Reprod Update.*2002 **8**, 559-577.

508 Dudek SM, Jacobson JR, Chiang ET, Birukov KG, Wang P, Zhan X, Garcia JG.
509 Pulmonary endothelial cell barrier enhancement by sphingosine 1-phosphate: roles for
510 cortactin and myosin light chain kinase. *J.Biol.Chem.*2004 **279**, 24692-24700.

511 Fiedler K, Ezcurra D. Predicting and preventing ovarian hyperstimulation syndrome
512 (OHSS): the need for individualized not standardized treatment.
513 *Reprod.Biol.Endocrinol.*2012 **10**, 32.

514 Fiedler U, Augustin HG. Angiopoietins: a link between angiogenesis and inflammation.
515 *Trends Immunol.*2006 **27**, 552-558.

516 Gaengel K, Niaudet C, Hagikura K, Lavina B, Muhl L, Hofmann JJ, Ebarasi L,
517 Nystrom S, Rymo S, Chen LL, Pang MF, Jin Y, Raschperger E, Roswall P, Schulte D,

518 Benedito R, Larsson J, Hellstrom M, Fuxe J, Uhlen P, Adams R, Jakobsson L,
519 Majumdar A, Vestweber D, Uv A, Betsholtz C. The sphingosine-1-phosphate receptor
520 S1PR1 restricts sprouting angiogenesis by regulating the interplay between VE-cadherin
521 and VEGFR2. *Dev.Cell*2012a **23**, 587-599.

522 Gaengel K, Niaudet C, Hagikura K, Lavina B, Muhl L, Hofmann JJ, Ebarasi L,
523 Nystrom S, Rymo S, Chen LL, Pang MF, Jin Y, Raschperger E, Roswall P, Schulte D,
524 Benedito R, Larsson J, Hellstrom M, Fuxe J, Uhlen P, Adams R, Jakobsson L,
525 Majumdar A, Vestweber D, Uv A, Betsholtz C. The sphingosine-1-phosphate receptor
526 S1PR1 restricts sprouting angiogenesis by regulating the interplay between VE-cadherin
527 and VEGFR2. *Dev.Cell*2012b **23**, 587-599.

528 Garcia JG, Liu F, Verin AD, Birukova A, Dechert MA, Gerthoffer WT, Bamberg JR,
529 English D. Sphingosine 1-phosphate promotes endothelial cell barrier integrity by Edg-
530 dependent cytoskeletal rearrangement. *J.Clin.Invest*2001 **108**, 689-701.

531 Golan A, Ron-El R, Herman A, Soffer Y, Weinraub Z, Caspi E. Ovarian
532 hyperstimulation syndrome: an update review. *Obstet.Gynecol.Surv.*1989 **44**, 430-440.

533 Gomez R, Soares SR, Busso C, Garcia-Velasco JA, Simon C, Pellicer A. Physiology
534 and pathology of ovarian hyperstimulation syndrome. *Semin.Reprod.Med.*2010 **28**, 448-
535 457.

536 Groten T, Fraser HM, Duncan WC, Konrad R, Kreienberg R, Wulff C. Cell junctional
537 proteins in the human corpus luteum: changes during the normal cycle and after HCG
538 treatment. *Hum.Reprod.*2006 **21**, 3096-3102.

539 Hanahan D, Folkman J. Patterns and emerging mechanisms of the angiogenic switch
540 during tumorigenesis. *Cell*1996 **86**, 353-364.

Hernandez F, Peluffo MC, Bas D, Stouffer RL, Tesone M. Local effects of the sphingosine 1-phosphate on prostaglandin F2alpha-induced luteolysis in the pregnant rat. *Mol.Reprod.Dev.*2009.

Herr D, Bekes I, Wulff C. Regulation of endothelial permeability in the primate corpora lutea: implications for ovarian hyperstimulation syndrome. *Reproduction.*2015 **149**, R71-R79.

Hoch RV, Soriano P. Roles of PDGF in animal development. *Development*2003 **130**, 4769-4784.

Irusta G, Parborell F, Peluffo M, Manna PR, Gonzalez-Calvar SI, Calandra R, Stocco DM, Tesone M. Steroidogenic acute regulatory protein in ovarian follicles of gonadotropin-stimulated rats is regulated by a gonadotropin-releasing hormone agonist. *Biol.Reprod.*2003 **68**, 1577-1583.

Irusta G, Parborell F, Tesone M. Inhibition of cytochrome P-450 C17 enzyme by a GnRH agonist in ovarian follicles from gonadotropin-stimulated rats. *Am.J Physiol Endocrinol.Metab*2007 **292**, E1456-E1464.

Jung B, Obinata H, Galvani S, Mendelson K, Ding BS, Skoura A, Kinzel B, Brinkmann V, Rafii S, Evans T, Hla T. Flow-regulated endothelial S1P receptor-1 signaling sustains vascular development. *Dev.Cell*2012 **23**, 600-610.

Kon J, Sato K, Watanabe T, Tomura H, Kuwabara A, Kimura T, Tamama K, Ishizuka T, Murata N, Kanda T, Kobayashi I, Ohta H, Ui M, Okajima F. Comparison of intrinsic activities of the putative sphingosine 1-phosphate receptor subtypes to regulate several signaling pathways in their cDNA-transfected Chinese hamster ovary cells. *J.Biol.Chem.*1999 **274**, 23940-23947.

564 Krump-Konvalinkova V, Yasuda S, Rubic T, Makarova N, Mages J, Erl W, Vosseler C,
565 Kirkpatrick CJ, Tigyi G, Siess W. Stable knock-down of the sphingosine 1-phosphate
566 receptor S1P1 influences multiple functions of human endothelial cells.
567 *Arterioscler.Thromb.Vasc.Biol.*2005 **25**, 546-552.

568 Le Stunff H, Peterson C, Thornton R, Milstien S, Mandala SM, Spiegel S.
569 Characterization of murine sphingosine-1-phosphate phosphohydrolase.
570 *J.Biol.Chem.*2002 **277**, 8920-8927.

571 Lee MJ, Thangada S, Claffey KP, Ancellin N, Liu CH, Kluk M, Volpi M, Sha'afi RI,
572 Hla T. Vascular endothelial cell adherens junction assembly and morphogenesis
573 induced by sphingosine-1-phosphate. *Cell*1999 **99**, 301-312.

574 Li F, Turan V, Lierman S, Cuvelier C, De Sutter P, Oktay K. Sphingosine-1-phosphate
575 prevents chemotherapy-induced human primordial follicle death. *Hum.Reprod.*2014 **29**,
576 107-113.

577 Liu X, Wu W, Li Q, Huang X, Chen B, Du J, Zhao K, Huang Q. Effect of sphingosine
578 1-phosphate on morphological and functional responses in endothelia and venules after
579 scalding injury. *Burns*2009 **35**, 1171-1179.

580 Mehta D, Konstantoulaki M, Ahmmed GU, Malik AB. Sphingosine 1-phosphate-
581 induced mobilization of intracellular Ca2+ mediates rac activation and adherens
582 junction assembly in endothelial cells. *J.Biol.Chem.*2005 **280**, 17320-17328.

583 Meng Y, Xu Z, Wu F, Chen W, Xie S, Liu J, Huang X, Zhou Y. Sphingosine-1-
584 phosphate suppresses cyclophosphamide induced follicle apoptosis in human fetal
585 ovarian xenografts in nude mice. *Fertil.Steril.*2014 **102**, 871-877.

586 Morita Y, Tilly JL. Sphingolipid regulation of female gonadal cell apoptosis.
587 *Ann.N.Y.Acad.Sci.*2000 **905**, 209-220.

588 Navot D, Bergh PA, Laufer N. Ovarian hyperstimulation syndrome in novel
589 reproductive technologies: prevention and treatment. *Fertil.Steril.*1992 **58**, 249-261.

590 Neufeld G, Cohen T, Gengrinovitch S, Poltorak Z. Vascular endothelial growth factor
591 (VEGF) and its receptors. *FASEB J.*1999 **13**, 9-22.

592 Niessen CM. Tight junctions/adherens junctions: basic structure and function. *J.Invest*
593 *Dermatol.*2007 **127**, 2525-2532.

594 Obinata H, Hla T. Sphingosine 1-phosphate in coagulation and inflammation.
595 *Semin.Immunopathol.*2012 **34**, 73-91.

596 Ogawa C, Kihara A, Gokoh M, Igarashi Y. Identification and characterization of a
597 novel human sphingosine-1-phosphate phosphohydrolase, hSPP2. *J.Biol.Chem.*2003
598 **278**, 1268-1272.

599 Olivera A, Rosenfeldt HM, Bektas M, Wang F, Ishii I, Chun J, Milstien S, Spiegel S.
600 Sphingosine kinase type 1 induces G12/13-mediated stress fiber formation, yet
601 promotes growth and survival independent of G protein-coupled receptors.
602 *J.Biol.Chem.*2003 **278**, 46452-46460.

603 Otrock ZK, Mahfouz RA, Makarem JA, Shamseddine AI. Understanding the biology of
604 angiogenesis: review of the most important molecular mechanisms. *Blood Cells*
605 *Mol.Dis.*2007 **39**, 212-220.

606 Paik JH, Skoura A, Chae SS, Cowan AE, Han DK, Proia RL, Hla T. Sphingosine 1-
607 phosphate receptor regulation of N-cadherin mediates vascular stabilization. *Genes*
608 *Dev.*2004 **18**, 2392-2403.

609 Pellicer A, Albert C, Mercader A, Bonilla-Musoles F, Remohi J, Simon C. The
610 pathogenesis of ovarian hyperstimulation syndrome: in vivo studies investigating the
611 role of interleukin-1beta, interleukin-6, and vascular endothelial growth factor.
612 *Fertil.Steril.*1999 **71**, 482-489.

613 Peng X, Hassoun PM, Sammani S, McVerry BJ, Burne MJ, Rabb H, Pearse D, Tuder
614 RM, Garcia JG. Protective effects of sphingosine 1-phosphate in murine endotoxin-
615 induced inflammatory lung injury. *Am.J.Respir.Crit Care Med.*2004 **169**, 1245-1251.

616 Potente M, Gerhardt H, Carmeliet P. Basic and therapeutic aspects of angiogenesis.
617 *Cell*2011 **146**, 873-887.

618 Redmer DA, Doraiswamy V, Bortnem BJ, Fisher K, Jablonka-Shariff A, Grazul-Bilska
619 AT, Reynolds LP. Evidence for a role of capillary pericytes in vascular growth of the
620 developing ovine corpus luteum. *Biol Reprod.*2001 **65**, 879-889.

621 Reynolds LP, Grazul-Bilska AT, Redmer DA. Angiogenesis in the corpus luteum.
622 *Endocrine.*2000 **12**, 1-9.

623 Risau W. Mechanisms of angiogenesis. *Nature*1997 **386**, 671-674.

624 Rizk B, Aboulghar M. Modern management of ovarian hyperstimulation syndrome.
625 *Hum.Reprod.*1991 **6**, 1082-1087.

626 Rodewald M, Herr D, Fraser HM, Hack G, Kreienberg R, Wulff C. Regulation of tight
627 junction proteins occludin and claudin 5 in the primate ovary during the ovulatory cycle

628 and after inhibition of vascular endothelial growth factor. *Mol.Hum.Reprod.*2007 **13**,
629 781-789.

630 Roth Z, Hansen PJ. Sphingosine 1-phosphate protects bovine oocytes from heat shock
631 during maturation. *Biol.Reprod.*2004 **71**, 2072-2078.

632 Sanchez T, Estrada-Hernandez T, Paik JH, Wu MT, Venkataraman K, Brinkmann V,
633 Claffey K, Hla T. Phosphorylation and action of the immunomodulator FTY720 inhibits
634 vascular endothelial cell growth factor-induced vascular permeability.
635 *J.Biol.Chem.*2003 **278**, 47281-47290.

636 Schneeberger EE, Lynch RD. The tight junction: a multifunctional complex.
637 *Am.J.Physiol Cell Physiol*2004 **286**, C1213-C1228.

638 Scotti L., Di Pietro M., Pascuali N., Irusta G., de Zúñiga I., Gomez Peña M., Pomilio C,
639 Saravia F., Tesone M., Abramovich D., Parborell F. Sphingosine-1- phosphate restores
640 endothelial barrier integrity in ovarian hyperstimulation syndrome. *Molecular Human*
641 *Reproduction*2016 in press.

642 Scotti L, Abramovich D, Pascuali N, de Z, I, Oubina A, Kopcow L, Lange S, Owen G,
643 Tesone M, Parborell F. Involvement of the ANGPTs/Tie-2 system in ovarian
644 hyperstimulation syndrome (OHSS). *Mol.Cell Endocrinol.*2013 **365**, 223-230.

645 Scotti L, Abramovich D, Pascuali N, Irusta G, Meresman G, Tesone M, Parborell F.
646 Local VEGF inhibition prevents ovarian alterations associated with ovarian
647 hyperstimulation syndrome. *J.Steroid Biochem.Mol.Biol.*2014a **144 Pt B**, 392-401.

Scotti L, Abramovich D, Pascuali N, Irusta G, Meresman G, Tesone M, Parborell F. Local VEGF inhibition prevents ovarian alterations associated with ovarian hyperstimulation syndrome. *J.Steroid Biochem.Mol.Biol.*2014b **144 Pt B**, 392-401.

Scotti L, Abramovich D, Pascuali N, Irusta G, Meresman G, Tesone M, Parborell F. Local VEGF inhibition prevents ovarian alterations associated with ovarian hyperstimulation syndrome. *J.Steroid Biochem.Mol.Biol.*2014c **144 Pt B**, 392-401.

Scotti L, Parborell F, Irusta G, de Z, I, Bisioli C, Pettorossi H, Tesone M, Abramovich D. Platelet-derived growth factor BB and DD and angiopoietin1 are altered in follicular fluid from polycystic ovary syndrome patients. *Mol.Reprod.Dev.*2014d **81**, 748-756.

Singleton PA, Dudek SM, Ma SF, Garcia JG. Transactivation of sphingosine 1-phosphate receptors is essential for vascular barrier regulation. Novel role for hyaluronan and CD44 receptor family. *J.Biol.Chem.*2006 **281**, 34381-34393.

Spiegel S, Milstien S. Sphingosine-1-phosphate: an enigmatic signalling lipid. *Nat.Rev.Mol.Cell Biol.*2003 **4**, 397-407.

Tillet E, Vittet D, Feraud O, Moore R, Kemler R, Huber P. N-cadherin deficiency impairs pericyte recruitment, and not endothelial differentiation or sprouting, in embryonic stem cell-derived angiogenesis. *Exp.Cell Res.*2005 **310**, 392-400.

Villasante A, Pacheco A, Ruiz A, Pellicer A, Garcia-Velasco JA. Vascular endothelial cadherin regulates vascular permeability: Implications for ovarian hyperstimulation syndrome. *J.Clin.Endocrinol.Metab*2007 **92**, 314-321.

Volk T, Geiger B. A 135-kd membrane protein of intercellular adherens junctions. *EMBO J.*1984 **3**, 2249-2260.

Walz A, Keck C, Weber H, Kissel C, Pietrowski D. Effects of luteinizing hormone and human chorionic gonadotropin on corpus luteum cells in a spheroid cell culture system. *Mol.Reprod.Dev.*2005 **72**, 98-104.

Wang C, Mao J, Redfield S, Mo Y, Lage JM, Zhou X. Systemic distribution, subcellular localization and differential expression of sphingosine-1-phosphate receptors in benign and malignant human tissues. *Exp.Mol.Pathol.*2014 **97**, 259-265.

Woodruff TK, D'Agostino J, Schwartz NB, Mayo KE. Dynamic changes in inhibin messenger RNAs in rat ovarian follicles during the reproductive cycle. *Science*1988 **239**, 1296-1299.

Xiong Y, Hla T. S1P control of endothelial integrity. *Curr.Top.Microbiol.Immunol.*2014 **378**, 85-105.

Yang L, Yatomi Y, Miura Y, Satoh K, Ozaki Y. Metabolism and functional effects of sphingolipids in blood cells. *Br.J.Haematol.*1999 **107**, 282-293.

Yatomi Y, Ruan F, Hakomori S, Igarashi Y. Sphingosine-1-phosphate: a platelet-activating sphingolipid released from agonist-stimulated human platelets. *Blood*1995 **86**, 193-202.

FIGURE LEGENDS

Figure 1: Effect of S1P treatment on preantral follicles, antral follicles, atretic follicles, corpora lutea and cysts from the rat OHSS model. The graphs show the percentage of each structure in H&E-stained ovarian sections. Different letters indicate significant differences. **(A)** % preantral follicles ($p>0.05$). **(B)** % antral follicles (Control vs OHSS $p<0.05$; OHSS vs OHSS+S1P $p<0.05$). **(C)** % atretic follicles

693 (p>0.05). **(D)** % corpora lutea (Control vs OHSS p<0.05; OHSS vs OHSS+S1P
694 p<0.01). **(E)** % cysts (Control vs OHSS p<0.001; Control vs OHSS+S1P p<0.01; OHSS
695 vs OHSS+S1P p<0.05). Data are expressed as the mean ± SEM. Results were obtained
696 from three experiments, using 6 rats per group.
697
698 **Figure 2: Effect of S1P treatment on steroidogenic enzymes levels in ovaries from**
699 **the rat OHSS model.** The levels of proteins in ovarian protein extracts were measured
700 by Western Blotting. The density in each band was normalized to the density of the β-
701 actin or GAPDH band. The lower panels show a representative blot for each protein
702 analyzed. Different letters indicate significant differences. **A)** 3βHSD (Control vs OHSS
703 p<0.05; Control vs OHSS+S1P p<0.05), **B)** P450scc (Control vs OHSS p<0.01; Control
704 vs OHSS+S1P p<0.01) and **C)** StAR (Control vs OHSS p<0.05; OHSS vs OHSS+S1P
705 p<0.05). Data are expressed as the mean ± SEM. Results were obtained from three
706 experiments, using 6 rats per group.
707
708 **Figure 3: Effect of S1P treatment on ovarian vessels-Corpora lutea from the rat**
709 **OHSS model. (A)** Lectin BS-1 staining in Control, OHSS, and S1P-treated OHSS rats.
710 Graph: Quantification of endothelial cell area in Corpora lutea sections stained in the
711 three groups analyzed. Different letters indicate significant differences (Control vs
712 OHSS p<0.001; OHSS vs OHSS+S1P p<0,001). The photographs show representative
713 histological sections of control, OHSS and OHSS+S1P Corpora lutea stained with lectin
714 BS-1. Scale bars, 100 μm. Three sections per ovary were analysed (six ovaries/group)
715 and at least four corpora lutea were photographed per section. **B)** Immunostaining of
716 periendothelial cells with anti-smooth muscle cell α-actin antibody in control, OHSS,
717 and S1P-treated OHSS rats. Graph: Quantification of periendothelial cell area in
718 Corpora lutea in the three groups analyzed. (Control vs OHSS p<0.001; OHSS vs

719 OHSS+S1P $p<0.05$; OHSS+S1P vs Control $p<0.01$). The photographs show
720 representative histological sections of control, OHSS, and S1P-treated OHSS rat ovaries
721 stained with anti-smooth muscle cell α-actin antibody. Scale bars, 100 μm. Three
722 sections per ovary were analysed (six ovaries/group) and at least four corpora lutea were
723 photographed per section
724
725 **Figure 4: Effect of S1P treatment on the expression of adherens and tight junction**
726 **proteins in ovaries from the rat OHSS model.** The graphs show the densitometric
727 analysis for adherens (N-cadherin and VE-cadherin) and tight (claudin-5, occludin,
728 Nectin-2) junction proteins in ovarian protein extracts. **A)** N-cadherin (Control vs
729 OHSS $p<0.05$; OHSS vs OHSS+S1P $p<0.05$), **B)** VE-cadherin (Control vs OHSS
730 $p<0.05$; OHSS vs OHSS+S1P $p<0.01$), **C)** claudin-5 (Control vs OHSS $p<0.01$; OHSS
731 vs OHSS+S1P $p<0.05$) **D)** occludin (Control vs OHSS $p<0.001$; Control vs OHSS+S1P
732 $p<0.05$; OHSS vs OHSS+S1P $p<0.05$) and **E)** Nectin-2 (Control vs OHSS $p<0.05$;
733 Control vs OHSS+S1P $p<0.05$). The density of each band was normalized to the density
734 of the β-actin or GAPDH band. The lower panels show a representative blot for each
735 protein analyzed. Different letters indicate significant differences. Data are expressed as
736 the mean ± SEM. Results were obtained from three experiments, using 6 rats per group.
737
738 **Figure 5: Effect of S1P treatment on the expression of S1P receptor 1 (S1PR1) in**
739 **ovaries from the rat OHSS model.** Densitometric quantification of S1PR1 levels in
740 ovarian protein extracts. The density of each band was normalized to the density of the
741 GAPDH band. The lower panels show a representative blot for the protein analyzed.
742 Different letters indicate significant differences (Control vs OHSS+S1P $p<0.01$; OHSS

743 vs OHSS+S1P p<0.01). Data are expressed as the mean ± SEM. Results were obtained
744 from three experiments, using 6 rats per group.
745
746 **Figure 6: Effect of S1P treatment on uterine morphology from the rat OHSS**
747 **model.** H&E stained sections show representative histological fields of Control, OHSS
748 and OHSS+S1P uterus. The dotted lines indicate the thickness of the endometrium. The
749 endometrium from the control group showed a few residual glands with a covering
750 epithelium that is low cuboidal to columnar. On the other hand, the endometrium of the
751 OHSS and S1P-treated OHSS group, showed a tall columnar surface epithelium with
752 pseudostratification and signs of an increased turnover, scattered glands are seen within
753 the thickness of the endometrium. Scale bars, 50 μm. Insets in all panels show images at
754 higher magnification of the endometrial epithelium. Scales bars, 5 μm.
755
756 **Table I: Effect of S1P treatment on ovarian weight and serum progesterone**
757 **concentration in a rat OHSS model.**

758	Control	OHSS
759 OHSS+S1P		
760	(n=6)	(n=6)
761 (n=6)		
762		
763 Ovarian weight (g)	0.057 ±0.003[a]	0.122±0.004[b]
764 0.093±0.007[c]		
765 Serum progesterone (ng/ml)	64.01±18.93[a]	173.70±15.31[b]
766 63.45±18.15[a]		

767 Note: Data are expressed as mean ± SEM; n = 6 rats/group. Letters indicate a significant
768 statistical difference between groups by one-way ANOVA, followed by Tukey's
769 multiple comparison test. Ovarian weight: a vs b P<0.001; a vs c P<0.01; b vs c P<0.05.
770 Serum progesterone: a vs b P < 0.001
771
772
773
774

OXFORD UNIVERSITY PRESS | Molecular Human Reproduction

In vivo intrabursal administration of bioactive lipid sphingosine-1-phosphate enhances vascular integrity in a rat model of ovarian hyperstimulation syndrome (OHSS)

Journal:	*Molecular Human Reproduction*
Manuscript ID	MHR-16-0224.R1
Manuscript Type:	Original Research
Date Submitted by the Author:	24-Jan-2017
Complete List of Authors:	Di Pietro, Mariana; Instituto de Biologia y Medicina Experimental Pascuali, Natalia; Instituto de Biologia y Medicina Experimental Scotti, Leopoldina; Instituto de Biologia y Medicina Experimental Irusta, Griselda; Instituto de Biologia y Medicina Experimental Bas, Diana; Instituto de Biologia y Medicina Experimental May, Maria; Instituto de Investigaciones Farmacológicas (ININFA-UBA-CONICET), Facultad de Farmacia y Bioquímica, Universidad de Buenos Aires Tesone, Marta; Instituto de Biologia y Medicina Experimental Abramovich, Dalhia; Instituto de Biologia y Medicina Experimental Parborell, FERNANDA; Instituto de Biologia y Medicina Experimental,
Key Words:	angiogenesis, ovary, OHSS, sphingolipids

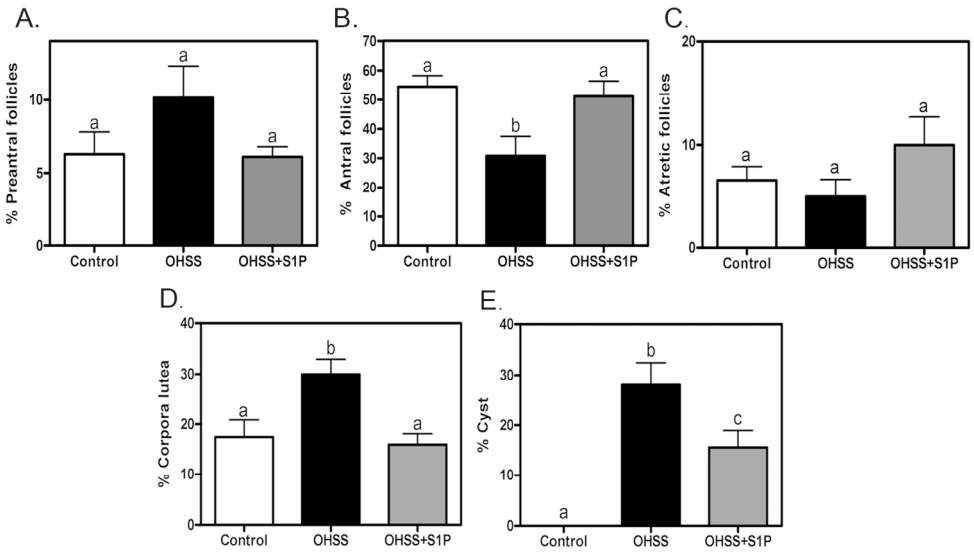

Figure 1: Effect of S1P treatment on preantral follicles, antral follicles, atretic follicles, corpora lutea and cysts from the rat OHSS model. The graphs show the percentage of each structure in H&E-stained ovarian sections. Different letters indicate significant differences. (A) % preantral follicles ($p>0.05$). (B) % antral follicles (Control vs OHSS $p<0.05$; OHSS vs OHSS+S1P $p<0.05$). (C) % atretic follicles ($p>0.05$). (D) % corpora lutea (Control vs OHSS $p<0.05$; OHSS vs OHSS+S1P $p<0.01$). (E) % cysts (Control vs OHSS $p<0.001$; Control vs OHSS+S1P $p<0.01$; OHSS vs OHSS+S1P $p<0.05$). Data are expressed as the mean±SEM. Results were obtained from three experiments, using 6 rats per group.

170x97mm (300 x 300 DPI)

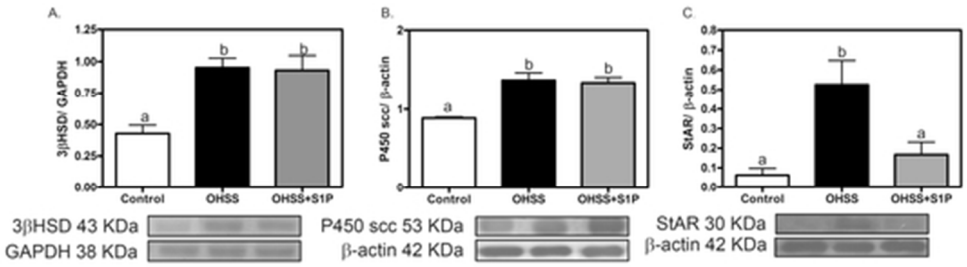

Figure 2: Effect of S1P treatment on steroidogenic enzymes levels in ovaries from the rat OHSS model. The levels of proteins in ovarian protein extracts were measured by Western Blotting. The density in each band was normalized to the density of the β-actin or GAPDH band. The lower panels show a representative blot for each protein analyzed. Different letters indicate significant differences. A) 3βHSD (Control vs OHSS $p<0.05$; Control vs OHSS+S1P $p<0.05$), B) P450 scc (Control vs OHSS $p<0.01$; Control vs OHSS+S1P $p<0.01$) and C) StAR (Control vs OHSS $p<0.05$; OHSS vs OHSS+S1P $p<0.05$). Data are expressed as the mean±SEM. Results were obtained from three experiments, using 6 rats per group.

46x12mm (300 x 300 DPI)

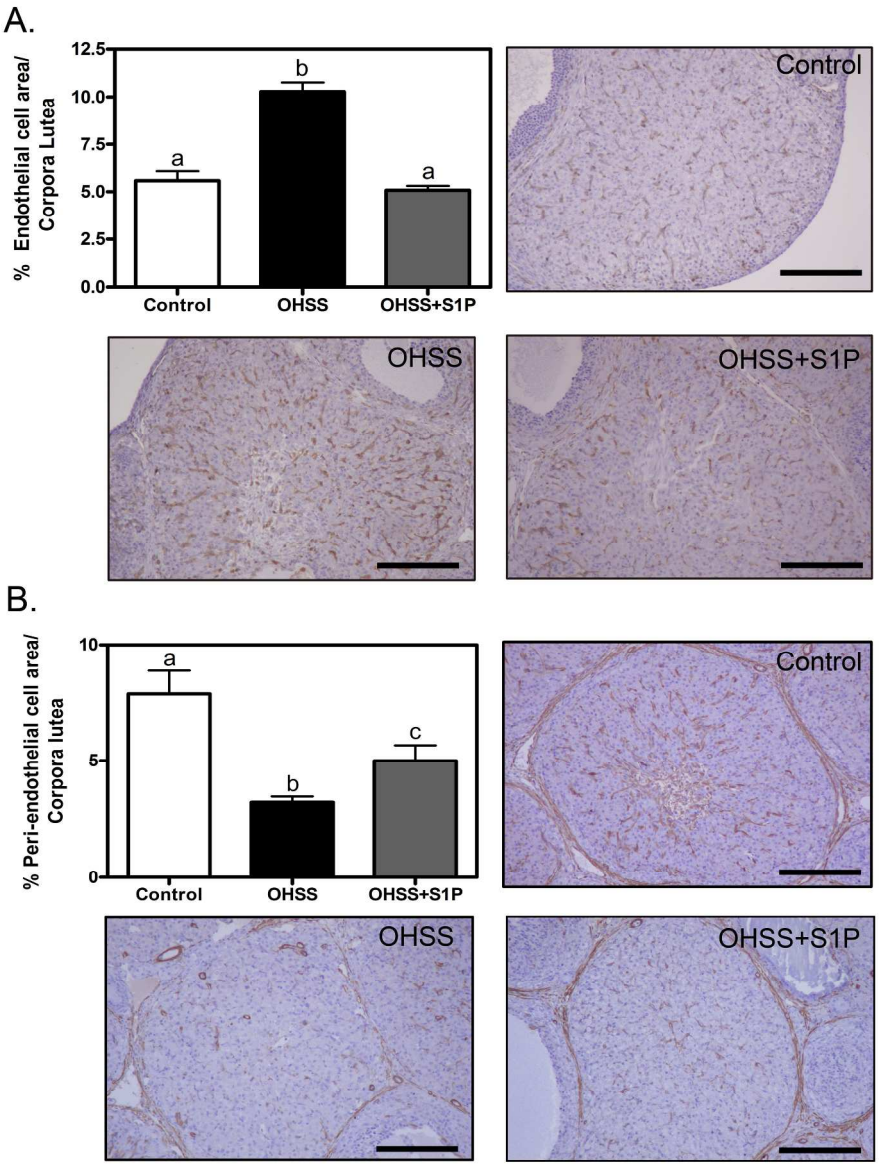

Figure 3: Effect of S1P treatment on ovarian vessels-Corpora lutea from the rat OHSS model. (A) Lectin BS-1 staining in Control, OHSS, and S1P-treated OHSS rats. Graph: Quantification of endothelial cell area in Corpora lutea sections stained in the three groups analyzed. Different letters indicate significant differences (Control vs OHSS $p<0.001$; OHSS vs OHSS+S1p $p<0,001$). The photographs show representative histological sections of control, OHSS and OHSS+S1P Corpora lutea stained with lectin BS-1. Scale bars, 100 μm. Three sections per ovary were analysed (six ovaries/group) and at least four corpora lutea were photographed per section. B) Immunostaining of periendothelial cells with anti-smooth muscle cell α-actin antibody in control, OHSS, and S1P-treated OHSS rats. Graph: Quantification of periendothelial cell area in Corpora lutea in the three groups analyzed. (Control vs OHSS $p<0.001$; OHSS vs OHSS+S1P $p<0.05$; OHSS+S1P vs Control $p<0.01$). The photographs show representative histological sections of control, OHSS, and S1P-treated OHSS rat ovaries stained with anti-smooth muscle cell α-actin antibody. Scale bars, 100 μm. Three sections per ovary were analysed (six ovaries/group) and at least four corpora lutea were photographed per section.

221x287mm (300 x 300 DPI)

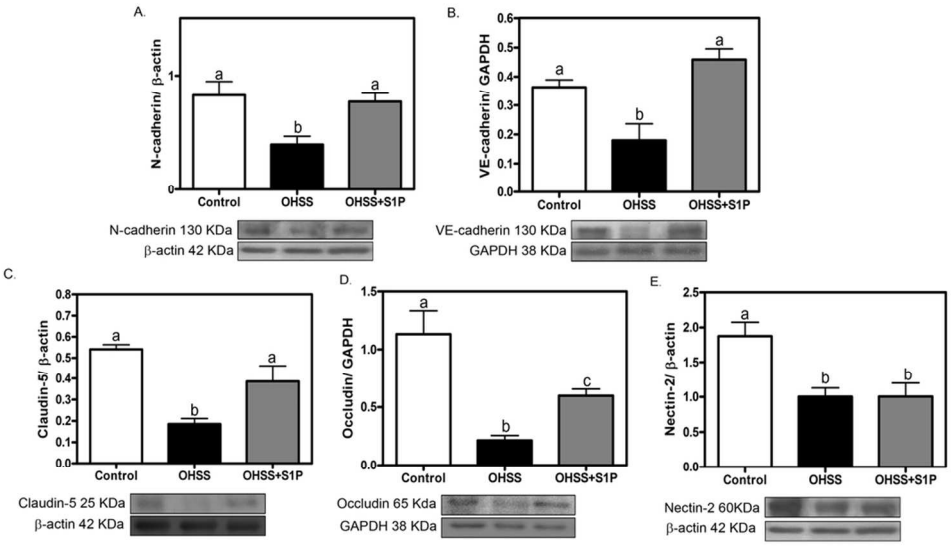

Figure 4: Effect of S1P treatment on the expression of adherens and tight junction proteins in ovaries from the rat OHSS model. The graphs show the densitometric analysis for adherens (N-cadherin and VE-cadherin) and tight (claudin-5, occludin, Nectin-2) junction proteins in ovarian protein extracts. A) N-cadherin (Control vs OHSS $p<0.05$; OHSS vs OHSS+S1P $p<0.05$), B) VE-cadherin (Control vs OHSS $p<0.05$; OHSS vs OHSS+S1P $p<0.01$), C) claudin-5 (Control vs OHSS $p<0.01$; OHSS vs OHSS+S1P $p<0.05$) D) occludin (Control vs OHSS $p<0.001$; Control vs OHSS+S1P $p<0.05$; OHSS vs OHSS+S1P $p<0.05$) and E) Nectin-2 (Control vs OHSS $p<0.05$; Control vs OHSS+S1P $p<0.05$). The density of each band was normalized to the density of the β-actin band. The lower panels show a representative blot for each protein analyzed. Different letters indicate significant differences. Data are expressed as the mean±SEM. Results were obtained from three experiments, using 6 rats per group.

95x53mm (300 x 300 DPI)

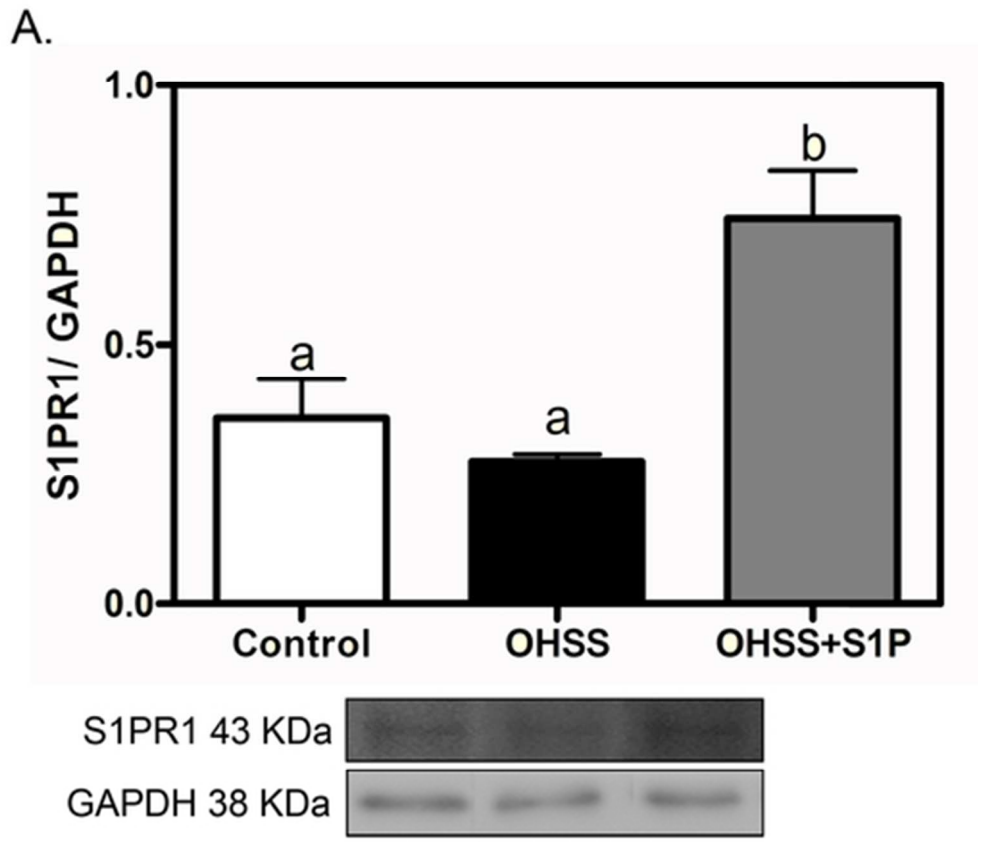

Figure 5: Effect of S1P treatment on the expression of S1P receptor 1 (S1PR1) in ovaries from the rat OHSS model. Densitometric quantification of S1PR1 levels in ovarian protein extracts. The density of each band was normalized to the density of the GAPDH band. The lower panels show a representative blot for the protein analyzed. Different letters indicate significant differences (Control vs OHSS+S1P $p<0.01$; OHSS vs OHSS+S1P $p<0.01$). Data are expressed as the mean±SEM. Results were obtained from three experiments, using 6 rats per group.

44x38mm (300 x 300 DPI)

TITLE PAGE

In vivo intrabursal administration of bioactive lipid sphingosine-1-phosphate enhances vascular integrity in a rat model of ovarian hyperstimulation syndrome (OHSS)

Running title: S1P restores the vascular integrity in OHSS.

Authors:

Mariana Di Pietro[1, ‡], Natalia Pascuali[1, ‡], Leopoldina Scotti[1], Griselda Irusta[1], Diana Bas[1], María May[3], Marta Tesone[1, 2], Dalhia Abramovich[1] and Fernanda Parborell[1]

[1] Instituto de Biología y Medicina Experimental (IByME) – CONICET, Buenos Aires, Argentina.

[2] Departamento de Química Biológica, Facultad de Ciencias Exactas y Naturales, Universidad de Buenos Aires, Buenos Aires, Argentina.

[3] Instituto de Investigaciones Farmacológicas (ININFA-UBA-CONICET), Facultad de Farmacia y Bioquímica, Universidad de Buenos Aires, Buenos Aires, Argentina.

‡Contributed equally

***Correspondence address:** e-mail: fparborell@gmail.com

ABSTRACT

Study question: Can the bioactive lipid sphingosine-1 phosphate (S1P) act as an endothelial barrier-enhancing molecule and, in turn, restore the vascular integrity and homeostasis in a rat model of ovarian hyperstimulation syndrome (OHSS).

Study answer: *In vivo* administration of S1P may prevent the early onset of OHSS and decrease its severity.

What is known already: Although advances in the prediction and treatment of OHSS have been made, complete prevention has not been possible yet. S1P in follicular fluid from women at risk of developing OHSS are lower in comparison from women who are not at such risk and administration of S1P in an OHSS rat model decreases ovarian capillary permeability.

Study design, size, duration: We used an animal model that develops OHSS in immature Sprague-Dawley rats. The rats were randomly divided into three groups: the control group, which was injected with 10 IU of pregnant mare's serum gonadotropin (PMSG), and 10 IU of human chorionic gonadotropin (hCG) 48 h later; the OHSS group, which was injected with excessive doses of PMSG (50 IU/day) for 4 consecutive days, followed by hCG; and the OHSS + S1P group, which was injected with the same doses of PMSG and hCG as the OHSS group and then treated with 5 µl S1P (1 mM) under the bursa of both ovaries, whereas the other groups of animals received the S1P vehicle.

Participants/materials, setting, methods: Rats were killed by decapitation 48 h after the hCG injection for ovary, endometrium and blood collection. The ovaries were weighed and then used for subsequent assays, while the serum was used for hormone assays. One of the ovaries from each rat (n=6) was used for Western immunoblot and the other for immunohistochemical analysis. Statistical comparisons between groups were carried out.

Main results and the role of chance: S1P administration reduced the ovarian weight ($p<0.05$), and decreased the concentration of serum progesterone in the OHSS group compared to the OHSS group without treatment ($p<0.001$). The percentage of antral follicles in the OHSS group was lower than that in the control group. S1P increased the percentage of antral follicles ($p<0.05$) and decreased the percentage of corpora lutea ($p<0.01$) and cystic structures in the OHSS group ($p<0.05$)**.** S1P had no effect on the expression levels of the enzymes 3β-hydroxysteroid dehydrogenase (3βHSD) or cholesterol side-chain cleavage enzyme (P450scc), but reduced the levels of steroidogenic acute regulatory protein (StAR) in OHSS rat ovaries. ($p<0.05$). S1P decreased the endothelial ($p<0.05$) and periendothelial ($p<0.01$) cell area in OHSS rat ovaries. S1P restored the levels of N-cadherin and VE-cadherin proteins to control values. Furthermore, S1P enhanced the levels of claudin-5, occludin ($p<0.05$) and sphingosine-1-phosphate receptor 1 (S1PR1) in OHSS ($p<0.01$). In addition, no histological differences were found in endometrium between OHSS and S1P-treated OHSS animals.

Limitations, reasons for caution: The results of this study were generated from an *in vivo* OHSS experimental model, which has been used by several authors and our group due to the similarity between the rat and human angiogenic systems. Further studies in patients will be needed to evaluate the effects of S1P in the pathogenesis of OHSS.

Wider implications of the findings: These findings concern the pathophysiological importance of S1P in OHSS. More studies on the regulation of endothelial cell barrier function by S1P in reproductive pathological processes and its therapeutic application are required.

Large scale data: N/A.

Study funding and competing interest(s): This work was supported by grants from ANPCyT (PICT 2012-897), CONICET (PIP 5471), Roemmers and Baron Foundations, Argentina. The authors declare no conflicts of interest.

Key words: angiogenesis, ovary, OHSS, sphingolipids, vascular integrity

INTRODUCTION

Ovarian hyperstimulation syndrome (OHSS) is one the most serious iatrogenic complications of follicular growth and maturation induced by ovulation induction. It is characterized by increased vascular leakage and ovarian enlargement, which cause fast third space fluid shifts from the intravascular compartment (Delvigne and Rozenberg 2002, Aboulghar and Mansour 2003). These shifts are caused by increased vascular permeability in response to stimulation with human chorionic gonadotropin (hCG) (Gomez *et al.,* 2010). The patho-physiology of OHSS is not completely understood, and no specific therapy or prevention is available yet (Rizk and Aboulghar 1991, Fiedler and Ezcurra 2012). It is recognized that this syndrome is triggered by hCG (Gomez *et al.,* 2010) and that the predominant link between hCG and OHSS is the production of angiogenic factors. Several pro-angiogenic factors, including members of the Vascular Endothelial Growth Factor A (VEGFA) family, angiopoietins (ANGPTs), transforming growth factors (TGFs), platelet-derived growth factors (PDGFs) and sphingosine-1 phosphate (S1P), have been identified (Neufeld *et al.,* 1999, Fiedler and Augustin 2006, Armulik *et al.,* 2005, Carmeliet 2000, Hanahan and Folkman 1996, Neufeld *et al.,* 1999, Otrock *et al.,* 2007, Allende and Proia 2002). One of the main functions of PDGFs and S1P, unlike VEGFA and ANGPTs, is the stabilization of newly developed capillaries (Hoch and Soriano 2003, Allende *et al.,* 2003, Xiong and Hla 2014).

Previously, we have evaluated the involvement of ANGPTs and PDGFs in this syndrome and we have observed that PDGF-B and -D protein levels decrease in ovaries from an OHSS rat model, while ANGPT2 and PDGFR-β levels remain constant (Scotti *et al.,* 2013). Furthermore, we have shown that ANGPT1 concentration is higher in follicular fluids (FF) from women at risk of developing OHSS than in FF from control patients, whilst the levels of the soluble form of the receptor Tie-2 (sTie-2) remain unchanged. Additionally, inhibition of ANGPT1 in FF from OHSS patients by the use of a neutralizing antibody decreases endothelial cell migration in comparison with untreated FF from OHSS women (Scotti *et al.,* 2013). Recently, we have observed that the levels of sphingolipid S1P in FF from women at risk of developing OHSS are lower in comparison with FF from women who are not at such risk, while the addition of S1P to the FF restores vascular integrity in an endothelial cell culture (Scotti L. *et al.,* 2016). Additionally, we have shown in the same study that *in vivo* intrabursal administration of S1P in an OHSS rat model decreased ovarian capillary permeability and ovarian expression of VEGF and its receptor KDR. All these findings suggest that the ANGPT, PDGF and S1P systems could be partly responsible for the characteristic increase in ovarian vascular permeability in OHSS.

S1P is derived from sphingosine phosphorylation by sphingosine kinase (Spiegel and Milstien 2003) and its degradation can be either mediated by S1P lyase (SPL) or by S1P phosphatases (Ogawa *et al.,* 2003, Le Stunff *et al.,* 2002). Not only is S1P secreted by activated platelets, but also erythrocytes, mononuclear cells, neutrophils and mastocytes can release this lipid mediator (Yatomi *et al.,* 1995, Yang *et al.,* 1999). S1P binds to specific cell surface receptors (S1PRs), which comprise a G-protein-coupled receptor family including subtypes S1PR1, S1P2, S1P3, S1P4 and S1P5. S1P is present in blood and plasma and delivered to its receptors by high-density lipoprotein (HDL)-associated apoliprotein M (Singleton *et al.,* 2006). S1P is a pleiotropic sphingolipid capable of modulating the

functions of various cell types (Xiong and Hla 2014). In particular, it regulates several physiological responses in vascular cells (Obinata and Hla 2012) and promotes endothelial cell spreading, vascular maturation/stabilization, and barrier function (Xiong and Hla 2014). The alteration of vascular barrier integrity causes serious consequences such as inflammation, edema, haemorrhage and ischemia. S1P has been proposed as a barrier-enhancing molecule and as a potential candidate for novel and specific therapies for endothelial dysfunction (Sanchez *et al.,* 2003, Jung *et al.,* 2012, Gaengel *et al.,* 2012b). In this regard, Dudek *et al.* (2004) and Liu *et al.* (2009) have shown that S1P administration in animal models with acute lung injury decreases vascular hyperpermeability by the enhancement of endothelial junctional integrity (Dudek *et al.,* 2004, Liu *et al.,* 2009). Furthermore, Curry *et al.* (2012) have previously shown that exogenous S1P attenuates acute microvascular permeability via receptor S1PR1 and stabilizes the endothelium in rats (Curry *et al.,* 2012).

The expression of S1PRs (S1PR1, S1P2 and S1P3) has been shown in female reproductive tissues and granulosa cells (Wang *et al.,* 2014, Kon *et al.,* 1999, Risau 1997). Also, several authors have previously documented the role of S1P in reproduction. Roth and Hansen (2004) have demonstrated that S1P may improve fertility when developmental competence of the oocytes is compromised (Roth and Hansen 2004). Other researchers have proposed S1P as a potential candidate for fertility preservation of female cancer patients (Li *et al.,* 2014, Meng *et al.,* 2014, Morita and Tilly 2000).

However, there are no studies on the effect of *in vivo* intrabursal S1P administration on ovarian morphology or vascular development and integrity in a rat model of OHSS. Therefore, the main purpose of this study was to evaluate the effects of local S1P administration on ovarian weight, follicular and luteal development, formation of cystic structures, steroidogenesis, endothelial and periendothelial area (pericytes and smooth

muscle cells), and on adherens and tight junction protein expression in ovaries from an OHSS rat model stimulated by equine chorionic gonadotropin (eCG), and hCG. In this model, we assessed the effect of S1P administration on S1PR1 protein expression in ovaries. Additionally, in this model we evaluated the effect of S1P on uterine morphology.

MATERIALS AND METHODS

Ethical approval

All procedures were approved by the ethics committee of the IByME (CE-018-2/2012) and conducted according to the guide for the care and use of laboratory animals of the National Institute of Health (USA).

Animal model and experimental design

Rats were housed and cared at the Instituto de Biología y Medicina Experimental (IByME), Buenos Aires, Argentina. Immature female Sprague-Dawley rats (21–23 days old) from our colony (n=6/group for each treatment) were allowed food and water *ad libitum* and kept at room temperature (21–23°C) on a 12L:12D cycle. We used an animal model that develops OHSS in immature Sprague-Dawley rats (21–23 days, 60–80 g), as described by Kitajima et al. (2004, 2006). The control group (n=6) was injected with 10 IU eCG and with 10 IU hCG 48 h later. The OHSS group (n=6) was injected with 50 IU eCG for four consecutive days, followed by 25 IU of hCG. The OHSS + S1P group (n=6) received the same doses of eCG and hCG as the OHSS group and was also treated with S1P. To administrate S1P on the day of hCG injection, the animals were anesthetized with ketamine HCl (70 mg/Kg; Holliday-Scott S.A., Buenos Aires, Argentina) and xylazine (5 mg/Kg; König Laboratories, Buenos Aires, Argentina) and the ovaries were exteriorized through an incision made in the dorsal lumbar region. The OHSS+S1P group received 5 µl S1P (1 mM) (Sigma Aldrich (St. Louis, MO, USA) under the bursa of both ovaries (Hernandez *et al.,* 2009), whereas the other

groups received the S1P vehicle (0.8% Tween-80; 2.5% ETOH; 5% polyethylene glycol (PEG).

Rats were killed by decapitation 48 h after the hCG injection for ovary and blood collection. The ovaries were removed and cleaned of adhering tissue in culture medium, weighed, and used for subsequent assays. The serum was used for hormone assays. One ovary from each rat (n=6) was used for Western blotting and the other for immunohistochemical analysis.

Steroid hormone assay

Serum steroid concentrations were measured by radioimmunoassay (RIA) (n=6 rats/group) (Irusta *et al.,* 2003, Irusta *et al.,* 2007). Progesterone (P_4) was measured by using specific antibodies supplied by Dr. G.D. Niswender (Animal Reproduction and Biotechnology Laboratory, Colorado State University, Fort Collins, CO, USA). Under these conditions, the intra- and inter-assay variations for P_4 were 8.0% and 14.2% respectively. The values are expressed per ml of serum.

Ovarian and endometrium morphology

Ovaries and uterine horns were extracted from the different experimental groups and immediately fixed in Bouin solution for 12 h. Histological sections were made for haematoxylin-eosin (H&E) staining. Ovarian sections (5 µm) were mounted at 50-µm intervals onto microscope slides to prevent counting the same structure twice, according to the method described by Woodruff *et al.* (Woodruff *et al.,* 1988). Preantral follicles, antral follicles, atretic follicles, corpora lutea (CL) and cystic structures were counted in six ovarian sections from each ovary (n=6 ovaries/group) and expressed as structure percentage per ovary. The total number of ovarian structures was defined as 100%. Cysts were defined as structures with presence of oocytes surrounded by luteal cells, remaining granulosa cells and

red blood cells (Scotti *et al.,* 2014c). A set of uterine sections was stained with H&E and examined microscopically by an experienced gynecologic pathologist, who was blinded to the group assignment.

Histochemistry and immunohistochemistry in luteal tissues

Tissue sections were deparaffinized in xylene and rehydrated by graduated ethanol washes. Endogenous peroxidase activity was blocked with hydrogen peroxide in PBS and nonspecific binding was blocked with 2% bovine serum albumin (BSA) overnight at 4ºC. Sections were incubated with biotinylated lectin BS-1 (from *Bandeiraea simplicifolia*, 20 µg/ml, Vector Laboratories, Burlingame, CA, USA) or α-SMA (smooth muscle actin) 1/250 (ab18147 Abcam, Cambridge, USA) overnight at 4ºC. Lectin BS-1 has demonstrated to be a constitutive endothelial cell marker staining endothelial cells at the different developmental stages of CL with similar intensity (Augustin *et al.,* 1995, Redmer *et al.,* 2001, Cherry *et al.,* 2008). After washing, slides were incubated with biotinylated anti-mouse IgG (except in the case of lectin BS-1) and afterwards with avidin-biotinylated horseradish peroxidase Complex (Vectastain ABC system from Vector Laboratories) for 30 min. Protein expression was visualized with diaminobenzidine (DAB) staining. After stopping the reaction with distilled water, slides were stained with haematoxylin, dehydrated and mounted (Canada Balsam Synthetic, Biopack, Argentina). Negative controls were obtained in absence of primary antibody.

The images were digitized with a camera (Nikon, Melville, NY, USA) mounted on a conventional light microscope (Nikon), using a magnification of 40X. Three sections per ovary were analysed (six ovaries/group) and at least four corpora lutea were photographed per section. Images were converted to TIFF format for analysis and processed using Image Pro-Plus 3.0 ® (Media Cybernetics, Silver Spring, MA, USA). Endothelial and peri-

endothelial cell areas were determined by thresholding each lectin BS-1- or α-SMA-positive stained areas, which were then normalised to the total area of the analysed corpus luteum.

Western blot

Ovaries were removed, placed on ice and resuspended in five volumes of lysis buffer (20 mM Tris-HCl pH 8, 137 mM NaCl, 1% Nonidet P-40 and 10% glycerol) supplemented with protease inhibitors (0.5 mM PMSF, 0.025 mM N-CBZ-$_L$-phenylalanine chloromethyl ketone, 0.025 mM N-p-tosyl-lysine chloromethyl ketone and 0.025 mM $_L$-1-tosylamide-2-phenyl-ethylchloromethyl ketone) and homogenized with an Ultra-Turrax homogenizer (IKA Werk, Breisgau, Germany). Samples were centrifuged at 4ºC for 10 min at 10,000 x g and the resulting pellets were discarded. Protein concentration in the supernatant was measured by the Bradford assay. After boiling for 5 min, 40 µg of protein was applied to a 12% SDS-polyacrylamide gel and electrophoresis was performed at 25 mA for 1.5 h. The resolved proteins were transferred onto nitrocellulose membranes for 2 h. The blot was then incubated in blocking buffer (5% nonfat milk, 0.05% tween-20 in 20 mM TBS pH 8.0) for 1 h at room temperature and incubated overnight at 4°C with appropriate primary antibodies: StAR 1/1000 was donated by Dr. D. M. Stocco (Texas Tech University Health Sciences Center); P450scc 1/2000 was donated by Dr. Anita Payne (Stanford University Medical Center, Stanford, CA, USA); S1PR1 (ab125074) was from Abcam (Cambridge, USA), 3βHSD 1/1000 (sc-30820), VE-cadherin 1/100 (sc-9989), N-cadherin 1/250 (sc-7939) and Nectin-2 1/200 (sc-373715) were from Santa Cruz Biotechnology, Inc. (Santa Cruz, CA, USA); and Claudin-5 1/1000 (35-2500), occludin: 1/1000 (71–1500) were from Invitrogen Corp. (Carlsbad, CA, USA), β-actin 1/10000 (4967) and GAPDH 1/10000 (14C10) were from Cell Signaling Technology, INC (Baverly, MA, USA). The blot was then incubated with anti-mouse or anti-rabbit secondary antibodies conjugated with horseradish peroxidase (1:1000)

and signal was detected by chemiluminescence. The protein levels were analysed by densitometry using Scion Image for Windows (Scion Corporation, Worman's Mill, CT, USA). Optical density data are expressed as arbitrary units ± SEM. The density in each band was normalised to the density of the β-actin or GAPDH band, which were used as an internal control.

Data analysis

The results are expressed as the mean ± SEM and the significant differences between groups were determined using analysis of variance (ANOVA), followed by Tukey's test. *P* values <0.05 were considered statistically significant. All samples were tested for normality before ANOVA. Data were statistically analysed using Prism v5.0.

RESULTS

Effect of S1P on ovarian weight and progesterone (P_4) concentration in the rat model of OHSS.

The effects of S1P on ovarian weight and P_4 serum concentration are summarized in Table I. The ovarian weight in the OHSS group was higher compared to the control group ($p<0.001$). S1P administration reduced the ovarian weight observed in the OHSS group without treatment ($p<0.05$). Serum P4 concentration in the OHSS group was higher than that in the control group ($p<0.001$). S1P treatment decreased the concentration of serum P_4 compared with the untreated OHSS group ($p<0.001$).

Effect of S1P on ovarian morphology and steroidogenic enzyme expression in the rat model of OHSS.

The percentage of antral follicles in the OHSS group was lower than that in the control group. In the OHSS+S1P group, the percentage of antral follicles increased compared to the OHSS group without treatment ($p<0.05$) (Fig. 1B). However, no significant differences were observed in the percentage of preantral or atretic follicles among the three experimental groups (Fig. 1A and C). The percentage of CL in the OHSS group increased significantly compared with that in the control group ($p<0.05$) (Fig. 1D). Local administration of S1P reduced the percentage of CL ($p<0.01$) and cystic structures in comparison with the untreated OHSS group ($p<0.05$) (Fig. 1D and E).

To evaluate the effect of S1P on steroidogenesis in the OHSS rat model, we studied the expression of 3βHSD, P450scc and StAR. The levels of these enzymes in the OHSS group were higher than those in the control group (3βHSD: $p<0.05$; P450scc: $p<0.01$; StAR: $p<0.05$) (Fig. 2). S1P administration had no effect on the expression levels of 3βHSD or P450scc in OHSS rat ovaries (Fig. 2A and B), but decreased StAR levels compared to the untreated OHSS group ($p<0.05$) (Fig. 2C).

Effect of S1P on luteal vascular development in the rat model of OHSS.

To evaluate whether S1P treatment causes changes on endothelial cells present in corpora lutea, we stained ovarian sections for lectin BS-1. The endothelial cell area in the OHSS group was higher than that in the control group ($p<0.001$), while S1P administration decreased the endothelial cell area compared to OHSS group ($p<0.001$) (Fig. 3A).

Also, we evaluated luteal vascular stability in ovarian sections immunostained with α-SMA antibody. The periendothelial cell area in the OHSS group was lower than that in the control group ($p<0.001$), while S1P increased the periendothelial cell area compared to the OHSS group without treatment ($p<0.05$) (Fig. 3B).

Effect of S1P on the expression of endothelial cell-to-cell junction proteins in the rat model of OHSS.

The levels of N-cadherin and VE-cadherin were lower in the OHSS group than in the control group ($p<0.05$). Local administration of S1P restored the levels of these proteins to control values (Fig. 4 A and B).

The levels of the tight junction proteins claudin-5, occludin and Nectin-2 were lower in the OHSS group in comparison with the control group (claudin-5: $p<0.01$; occludin: $p<0.001$; Nectin-2: $p<0.05$). S1P treatment increased the levels of claudin-5 and occludin compared to those in the OHSS group ($p<0.05$), whereas the levels of Nectin-2 remained unchanged (Fig. 4 C, D and E).

Effect of S1P on the expression of S1PR1 in the rat model of OHSS.

The ovarian levels of S1PR1 in the OHSS group were similar to those in the control group. In the OHSS+S1P group, the levels of S1PR1 increased compared to those of the OHSS group ($p<0.01$) (Fig. 5).

Effect of S1P on uterine morphology in the rat model of OHSS

The endometrium from the control group showed a few residual glands surrounded by an atrophic, somewhat fibrotic stroma. The epithelium was low cuboidal or columnar with almost no mitotic figures (Fig. 6).

The endometrium of the OHSS and S1P-treated OHSS groups showed a columnar surface epithelium with slight pseudostratification and small, round and regular glands. In addition, endometrial stroma showed no edema but occasional mitotic figures, and small and regularly

distributed blood vessels. No histological differences were found in endometrium between OHSS and S1P-treated OHSS animals.

DISCUSSION

The main clinical characteristics of OHSS are ovarian enlargement, with luteal and haemorrhagic cysts, and increased vascular permeability (Golan *et al.,* 1989, Gomez *et al.,* 2010). Previously, we and other authors have demonstrated that VEGF, ANGPTs, PDGFs could be mediators in the development of OHSS (Artini *et al.,* 1998, Pellicer *et al.,* 1999, Scotti *et al.,* 2014d, Scotti *et al.,* 2014b, Scotti *et al.,* 2013). Recently, we have shown that S1P levels are lower in FF from patients at risk of OHSS and that treatment with S1P may decrease vascular permeability in these patients (Scotti L. *et al.,* 2016).

In the current study, we present evidence for the first time that S1P intrabursal administration *in vivo* affects ovarian weight, follicular and luteal development, formation of cystic structures and steroidogenesis in ovaries from a rat OHSS model. Additionally, we observed that local administration of this sphingolipid causes a decrease in the endothelial area, an increase in both the peri-endothelial area and N-cadherin, VE-cadherin, claudin-5 and S1PR1 receptor protein levels in the ovaries of the above-mentioned model.

In humans, OHSS generates the formation of multiple CL and the increase of VEGF levels (Navot *et al.,* 1992). Our study is the first to demonstrate that administration of S1P *in vivo* in ovaries from OHSS rats affects luteal development, delays folliculogenesis and leads to a lower percentage of CL. These results suggest that, as S1P decreases the presence of CL, which secrete several angiogenic factors that in turn favour an altered angiogenesis, this lipid metabolite is also likely to ameliorate the vascular permeability observed in OHSS. The decrease in CL and cystic structures in the S1P-treated ovaries is consistent with the decrease in serum P_4 and ovarian weight observed. It is known that the transport of cholesterol from

345 the cytoplasm to the inner mitochondrial membrane, mediated by the StAR protein, is the
346 limiting step in progesterone (P_4) synthesis. Therefore, the diminished expression of StAR, as
347 demonstrated by Western blot, could be partly responsible for the decrease in serum P_4 in the
348 S1P-treated OHSS rats. These results are consistent with those obtained by other authors
349 such as Budnik *et al.* (2005), who have shown that S1P suppresses P_4 synthesis in luteal cells
350 and Leydig tumour cells stimulated with luteotropic hormone or a cAMP analog (Budnik and
351 Brunswig-Spickenheier 2005). It is worth noting that S1P did not affect ovarian expression of
352 P450scc or 3βHSD, which are critical for biosynthesis of steroid hormones.
353 CL are highly vascularized structures, whose vascular development exceeds that of most
354 tumours (Reynolds *et al.,* 2000). In this study, the *in vivo* administration of S1P may have
355 altered the formation and function of CL by preventing angiogenesis in OHSS. The decrease
356 in luteal endothelial cell area after S1P administration suggests that the sphingolipid caused a
357 decrease in the number of endothelial cells, and thus a decrease in the luteal microvasculature
358 that likely contributed to the decrease in serum P_4 concentrations. Pericyte coverage induces
359 vessel maturation by resolving angiogenic signals and reducing endothelial proliferation.
360 Thus, the recruitment of peri-endothelial cells and the deposition of basal membranes
361 represent crucial steps to achieve vascular maturation (Potente *et al.,* 2011). In our study,
362 S1P was able to increase the recruitment of pericytes and smooth muscle cells, enhancing
363 pericyte-endothelium interaction and, in turn, improving luteal vessel stability in OHSS. It is
364 worth noting that the breakdown of the S1P signalling system results in pathological
365 hyperpermeability such as acute lung injury, anaphylaxis and inflammation (Peng *et al.,*
366 2004, Olivera *et al.,* 2003).
367 Controlled dynamic changes in the localization and expression of adhesion molecules are
368 essential in the ovary (Groten *et al.,* 2006, Rodewald *et al.,* 2007). This includes regulation
369 of adherens and tight junctions (AJ and TJ), which are key components of intercellular

junctions (Dejana 2004, Schneeberger and Lynch 2004). An increase in endothelial permeability is generally accompanied by reorganization of junctional proteins, inducing a transient opening of the endothelial junctions and an increment in vascular permeability (Bazzoni and Dejana 2004, Dejana 2004, Walz *et al.,* 2005). TJ proteins, which are composed of at least three different families of transmembrane proteins (claudins, occludins and junction adhesion molecules), represent a barrier to molecule diffusion from the vessel lumen to the tissue parenchyma (Groten *et al.,* 2006), whereas AJ proteins involve transmembrane proteins belonging to the cadherin family. Thus, we propose that TJ and AJ proteins are downstream targets of S1P in vascular cells of ovaries from animals with OHSS. Since VE-cadherin is the main structural protein of AJ in endothelial cells (Mehta *et al.,* 2005), we decided to study the levels of this protein in the OHSS rat model. We and other authors showed the importance of this cadherin in the development of OHSS (Villasante *et al.,* 2007, Scotti *et al.,* 2014a). We have previously observed that VE-cadherin levels decrease significantly in endothelial cells incubated with FF from OHSS patients compared to control patients. In the present study, we observed that S1P is able to restore the levels of VE-cadherin, contributing to the sealing of the intercellular space and reducing vascular permeability in the ovary. These results are consistent with recently obtained studies in our laboratory, as we found that S1P addition increased VE-cadherin expression and reduced VEGF expression in endothelial cells compared to FF from patients at risk of OHSS without the sphingolipid (Scotti L. *et al.,* 2016). Regarding this point, Gaengel *et al.* (2012) have studied the communication between the VEGF and S1P systems and demonstrated that when co-stimulating human umbilical vein endothelial cells (HUVEC) with VEGF and S1P, VE-cadherin remained stable in endothelial junctions and was insensitive to the internalization induced by VEGF (Gaengel et al., 2012). Additionally, Lee *et al.* (1999) have demonstrated that S1P increases the VE-cadherin and β-catenin levels and, in turn, enhances AJ assembly

in confluent HUVEC (Lee *et al.,* 1999). Furthermore, Krump-Konvalinkova *et al.* (2005) have shown that S1PR1 silencing decreases the expression of platelet-endothelial cell adhesion molecule-1 (PECAM) and VE-cadherin human endothelial cell lines (Krump-Konvalinkova *et al.,* 2005).

Besides VE-cadherin, N-cadherin also regulates vascular stability since it mediates pericyte adhesion to endothelial cells, enhancing vessel maturation and stabilization (Volk and Geiger 1984, Tillet *et al.,* 2005). In the present study, S1P restored the levels of N-cadherin suggesting that, in OHSS, S1P improves the endothelial-pericyte interaction mediated by this cadherin, contributing to vessel maturation and endothelial barrier integrity. This supports previous data from our laboratory, where we have shown that S1P addition increased N-cadherin levels in endothelial cells compared to FF from patients at risk of OHSS without the sphingolipid (Scotti L. *et al.,* 2016). Furthermore, Paik *et al.* (2004) have shown that the inhibition of N-cadherin affects vascular stabilization *in vitro* and *in vivo*, suggesting a specific involvement of S1P in N-cadherin-induced pericyte attachment (Paik *et al.,* 2004).

The nectin system has been described as a novel modulator of AJ and TJ, and provides the first scaffold for the formation of these junctions (Niessen 2007). Based on this information, we analysed the expression in the rat OHSS model of claudin-5 and occludin (TJ proteins), and also of nectin-2, the only member of the nectin system that is expressed in the endothelium of CL (Herr *et al.,* 2015). S1P was able to restore the decreased levels of claudin-5, occludin and nectin 2, contributing to the formation of TJ and ovarian vascular stability. Taking together these results suggests that S1P upregulates VE-cadherin, N-cadherin, claudin-5 and occludin and consequently reduces vascular permeability in OHSS. Accordingly, S1P improves the assembly of AJ and assists in the formation of TJ.

Moreover, S1P is able to enhance endothelial maturation through its receptor, S1PR1, by promoting Rac1 activation and AJ assembly (Garcia *et al.,* 2001). Thus, we evaluated

S1PR1 expression in the OHSS model. S1P was able to upregulate the expression of its own receptor, enhancing vascular integrity and, in turn, avoiding the aberrant angiogenic responses observed in OHSS. The precise mechanism by which the sphingolipid increases expression of its own receptor is currently unknown. These findings are in line with the observations by Gaengel *et al*. (2003), who demonstrated that S1PR1 signalling inhibits endothelial hyper-sprouting through stabilization of VE-cadherin and through inhibition of VEGFR2 phosphorylation (Gaengel *et al.,* 2012a).

We decided to evaluate possible side-effects of S1P treatment in other vascularized organs, such as the uterus. We did not observe any change in endometrial morphology after S1P treatment in the OHSS model.

In summary, our study shows that local S1P administration decreases the percentage of CL and cystic structures, serum P_4 concentrations, endothelial cell area, and StAR protein expression in ovaries from OHSS rats, and increases the percentage of antral follicles, peri-endothelial area, and S1PR1, AJ and TJ protein levels in OHSS rats.

Therefore, local administration of S1P decreased the vascular permeability and angiogenesis in the OHSS group. These effects would be directly mediated by the decrease in the percentage of the CL and in blood vessel development, and by the increase in vascular stability in the CL. Our findings would indicate for the first time that S1P acts in the rat OHSS model as an endothelial barrier-enhancing factor, restoring the vascular integrity and homeostasis in OHSS. S1P administration may therefore prevent the early onset of OHSS and decrease its severity. More studies on the regulation of endothelial cell barrier function by the bioactive lipid S1P in reproductive pathological processes and its therapeutic application are required.

Acknowledgements

We thank ANPCyT (PICT 2012-897), CONICET (PIP 5471), Roemmers Foundation and René Barón Foundation, Argentina, for supporting the study.

Authors' Roles

MD and NP performed the experiments and contributed to data analysis and interpretation.

LS discussed the results and helped draft the manuscript.

DB, GI and MT contributed to data interpretation and discussed the results.

DA analysed and discussed the results, and helped draft the manuscript.

MM performed the assessment of uterine morphology.

FP conceived the concept, designed the experiments, supervised the study and wrote the manuscript.

All the authors read and approved the final manuscript.

Funding

This study was supported by grants ANPCyT (PICT 2012-897), CONICET (PIP 5471), and Roemmers and Baron Foundations, Argentina.

Conflict of interest

The authors declare no potential conflicts of interest with respect to the research, authorship, and/or publication of this article.

REFERENCES

Aboulghar MA, Mansour RT. Ovarian hyperstimulation syndrome: classifications and critical analysis of preventive measures. *Hum.Reprod.Update.*2003 **9**, 275-289.

Allende ML, Proia RL. Sphingosine-1-phosphate receptors and the development of the vascular system. *Biochim.Biophys.Acta*2002 **1582**, 222-227.

Allende ML, Yamashita T, Proia RL. G-protein-coupled receptor S1P1 acts within endothelial cells to regulate vascular maturation. *Blood*2003 **102**, 3665-3667.

Armulik A, Abramsson A, Betsholtz C. Endothelial/pericyte interactions. *Circ.Res.*2005 **97**, 512-523.

Artini PG, Monti M, Fasciani A, Tartaglia ML, D'Ambrogio G, Genazzani AR. Correlation between the amount of follicle-stimulating hormone administered and plasma and follicular fluid vascular endothelial growth factor concentrations in women undergoing in vitro fertilization. *Gynecol.Endocrinol.*1998 **12**, 243-247.

Augustin HG, Braun K, Telemenakis I, Modlich U, Kuhn W. Ovarian angiogenesis. Phenotypic characterization of endothelial cells in a physiological model of blood vessel growth and regression. *Am.J.Pathol.*1995 **147**, 339-351.

Bazzoni G, Dejana E. Endothelial cell-to-cell junctions: molecular organization and role in vascular homeostasis. *Physiol Rev.*2004 **84**, 869-901.

Budnik LT, Brunswig-Spickenheier B. Differential effects of lysolipids on steroid synthesis in cells expressing endogenous LPA2 receptor. *J.Lipid Res.*2005 **46**, 930-941.

Carmeliet P. Fibroblast growth factor-1 stimulates branching and survival of myocardial arteries: a goal for therapeutic angiogenesis? *Circ.Res.*2000 **87**, 176-178.

491 Cherry JA, Hou X, Rueda BR, Davis JS, Townson DH. Microvascular endothelial cells
492 of the bovine corpus luteum: a comparative examination of the estrous cycle and
493 pregnancy. *J.Reprod.Dev.*2008 **54**, 183-191.

494 Curry FE, Clark JF, Adamson RH. Erythrocyte-derived sphingosine-1-phosphate
495 stabilizes basal hydraulic conductivity and solute permeability in rat microvessels.
496 *Am.J.Physiol Heart Circ.Physiol*2012 **303**, H825-H834.

497 Dejana E. Endothelial cell-cell junctions: happy together. *Nat.Rev.Mol.Cell Biol*2004 **5**,
498 261-270.

499 Delvigne A, Rozenberg S. Epidemiology and prevention of ovarian hyperstimulation
500 syndrome (OHSS): a review. *Hum.Reprod Update.*2002 **8**, 559-577.

501 Dudek SM, Jacobson JR, Chiang ET, Birukov KG, Wang P, Zhan X, Garcia JG.
502 Pulmonary endothelial cell barrier enhancement by sphingosine 1-phosphate: roles for
503 cortactin and myosin light chain kinase. *J.Biol.Chem.*2004 **279**, 24692-24700.

504 Fiedler K, Ezcurra D. Predicting and preventing ovarian hyperstimulation syndrome
505 (OHSS): the need for individualized not standardized treatment.
506 *Reprod.Biol.Endocrinol.*2012 **10**, 32.

507 Fiedler U, Augustin HG. Angiopoietins: a link between angiogenesis and inflammation.
508 *Trends Immunol.*2006 **27**, 552-558.

509 Gaengel K, Niaudet C, Hagikura K, Lavina B, Muhl L, Hofmann JJ, Ebarasi L,
510 Nystrom S, Rymo S, Chen LL, Pang MF, Jin Y, Raschperger E, Roswall P, Schulte D,
511 Benedito R, Larsson J, Hellstrom M, Fuxe J, Uhlen P, Adams R, Jakobsson L,
512 Majumdar A, Vestweber D, Uv A, Betsholtz C. The sphingosine-1-phosphate receptor

513 S1PR1 restricts sprouting angiogenesis by regulating the interplay between VE-cadherin
514 and VEGFR2. *Dev.Cell*2012a **23**, 587-599.

515 Gaengel K, Niaudet C, Hagikura K, Lavina B, Muhl L, Hofmann JJ, Ebarasi L,
516 Nystrom S, Rymo S, Chen LL, Pang MF, Jin Y, Raschperger E, Roswall P, Schulte D,
517 Benedito R, Larsson J, Hellstrom M, Fuxe J, Uhlen P, Adams R, Jakobsson L,
518 Majumdar A, Vestweber D, Uv A, Betsholtz C. The sphingosine-1-phosphate receptor
519 S1PR1 restricts sprouting angiogenesis by regulating the interplay between VE-cadherin
520 and VEGFR2. *Dev.Cell*2012b **23**, 587-599.

521 Garcia JG, Liu F, Verin AD, Birukova A, Dechert MA, Gerthoffer WT, Bamberg JR,
522 English D. Sphingosine 1-phosphate promotes endothelial cell barrier integrity by Edg-
523 dependent cytoskeletal rearrangement. *J.Clin.Invest*2001 **108**, 689-701.

524 Golan A, Ron-El R, Herman A, Soffer Y, Weinraub Z, Caspi E. Ovarian
525 hyperstimulation syndrome: an update review. *Obstet.Gynecol.Surv.*1989 **44**, 430-440.

526 Gomez R, Soares SR, Busso C, Garcia-Velasco JA, Simon C, Pellicer A. Physiology
527 and pathology of ovarian hyperstimulation syndrome. *Semin.Reprod.Med.*2010 **28**, 448-
528 457.

529 Groten T, Fraser HM, Duncan WC, Konrad R, Kreienberg R, Wulff C. Cell junctional
530 proteins in the human corpus luteum: changes during the normal cycle and after HCG
531 treatment. *Hum.Reprod.*2006 **21**, 3096-3102.

532 Hanahan D, Folkman J. Patterns and emerging mechanisms of the angiogenic switch
533 during tumorigenesis. *Cell*1996 **86**, 353-364.

534 Hernandez F, Peluffo MC, Bas D, Stouffer RL, Tesone M. Local effects of the
535 sphingosine 1-phosphate on prostaglandin F2alpha-induced luteolysis in the pregnant
536 rat. *Mol.Reprod.Dev.*2009.

537 Herr D, Bekes I, Wulff C. Regulation of endothelial permeability in the primate corpora
538 lutea: implications for ovarian hyperstimulation syndrome. *Reproduction.*2015 **149**,
539 R71-R79.

540 Hoch RV, Soriano P. Roles of PDGF in animal development. *Development*2003 **130**,
541 4769-4784.

542 Irusta G, Parborell F, Peluffo M, Manna PR, Gonzalez-Calvar SI, Calandra R, Stocco
543 DM, Tesone M. Steroidogenic acute regulatory protein in ovarian follicles of
544 gonadotropin-stimulated rats is regulated by a gonadotropin-releasing hormone agonist.
545 *Biol.Reprod.*2003 **68**, 1577-1583.

546 Irusta G, Parborell F, Tesone M. Inhibition of cytochrome P-450 C17 enzyme by a
547 GnRH agonist in ovarian follicles from gonadotropin-stimulated rats. *Am.J Physiol*
548 *Endocrinol.Metab*2007 **292**, E1456-E1464.

549 Jung B, Obinata H, Galvani S, Mendelson K, Ding BS, Skoura A, Kinzel B, Brinkmann
550 V, Rafii S, Evans T, Hla T. Flow-regulated endothelial S1P receptor-1 signaling
551 sustains vascular development. *Dev.Cell*2012 **23**, 600-610.

552 Kon J, Sato K, Watanabe T, Tomura H, Kuwabara A, Kimura T, Tamama K, Ishizuka
553 T, Murata N, Kanda T, Kobayashi I, Ohta H, Ui M, Okajima F. Comparison of intrinsic
554 activities of the putative sphingosine 1-phosphate receptor subtypes to regulate several
555 signaling pathways in their cDNA-transfected Chinese hamster ovary cells.
556 *J.Biol.Chem.*1999 **274**, 23940-23947.

557 Krump-Konvalinkova V, Yasuda S, Rubic T, Makarova N, Mages J, Erl W, Vosseler C,
558 Kirkpatrick CJ, Tigyi G, Siess W. Stable knock-down of the sphingosine 1-phosphate
559 receptor S1P1 influences multiple functions of human endothelial cells.
560 *Arterioscler.Thromb.Vasc.Biol.*2005 **25**, 546-552.

561 Le Stunff H, Peterson C, Thornton R, Milstien S, Mandala SM, Spiegel S.
562 Characterization of murine sphingosine-1-phosphate phosphohydrolase.
563 *J.Biol.Chem.*2002 **277**, 8920-8927.

564 Lee MJ, Thangada S, Claffey KP, Ancellin N, Liu CH, Kluk M, Volpi M, Sha'afi RI,
565 Hla T. Vascular endothelial cell adherens junction assembly and morphogenesis
566 induced by sphingosine-1-phosphate. *Cell*1999 **99**, 301-312.

567 Li F, Turan V, Lierman S, Cuvelier C, De Sutter P, Oktay K. Sphingosine-1-phosphate
568 prevents chemotherapy-induced human primordial follicle death. *Hum.Reprod.*2014 **29**,
569 107-113.

570 Liu X, Wu W, Li Q, Huang X, Chen B, Du J, Zhao K, Huang Q. Effect of sphingosine
571 1-phosphate on morphological and functional responses in endothelia and venules after
572 scalding injury. *Burns*2009 **35**, 1171-1179.

573 Mehta D, Konstantoulaki M, Ahmmed GU, Malik AB. Sphingosine 1-phosphate-
574 induced mobilization of intracellular Ca2+ mediates rac activation and adherens
575 junction assembly in endothelial cells. *J.Biol.Chem.*2005 **280**, 17320-17328.

576 Meng Y, Xu Z, Wu F, Chen W, Xie S, Liu J, Huang X, Zhou Y. Sphingosine-1-
577 phosphate suppresses cyclophosphamide induced follicle apoptosis in human fetal
578 ovarian xenografts in nude mice. *Fertil.Steril.*2014 **102**, 871-877.

579 Morita Y, Tilly JL. Sphingolipid regulation of female gonadal cell apoptosis.
580 *Ann.N.Y.Acad.Sci.*2000 **905**, 209-220.

581 Navot D, Bergh PA, Laufer N. Ovarian hyperstimulation syndrome in novel
582 reproductive technologies: prevention and treatment. *Fertil.Steril.*1992 **58**, 249-261.

583 Neufeld G, Cohen T, Gengrinovitch S, Poltorak Z. Vascular endothelial growth factor
584 (VEGF) and its receptors. *FASEB J.*1999 **13**, 9-22.

585 Niessen CM. Tight junctions/adherens junctions: basic structure and function. *J.Invest*
586 *Dermatol.*2007 **127**, 2525-2532.

587 Obinata H, Hla T. Sphingosine 1-phosphate in coagulation and inflammation.
588 *Semin.Immunopathol.*2012 **34**, 73-91.

589 Ogawa C, Kihara A, Gokoh M, Igarashi Y. Identification and characterization of a
590 novel human sphingosine-1-phosphate phosphohydrolase, hSPP2. *J.Biol.Chem.*2003
591 **278**, 1268-1272.

592 Olivera A, Rosenfeldt HM, Bektas M, Wang F, Ishii I, Chun J, Milstien S, Spiegel S.
593 Sphingosine kinase type 1 induces G12/13-mediated stress fiber formation, yet
594 promotes growth and survival independent of G protein-coupled receptors.
595 *J.Biol.Chem.*2003 **278**, 46452-46460.

596 Otrock ZK, Mahfouz RA, Makarem JA, Shamseddine AI. Understanding the biology of
597 angiogenesis: review of the most important molecular mechanisms. *Blood Cells*
598 *Mol.Dis.*2007 **39**, 212-220.

599 Paik JH, Skoura A, Chae SS, Cowan AE, Han DK, Proia RL, Hla T. Sphingosine 1-
600 phosphate receptor regulation of N-cadherin mediates vascular stabilization. *Genes*
601 *Dev.*2004 **18**, 2392-2403.

602 Pellicer A, Albert C, Mercader A, Bonilla-Musoles F, Remohi J, Simon C. The
603 pathogenesis of ovarian hyperstimulation syndrome: in vivo studies investigating the
604 role of interleukin-1beta, interleukin-6, and vascular endothelial growth factor.
605 *Fertil.Steril.*1999 **71**, 482-489.

606 Peng X, Hassoun PM, Sammani S, McVerry BJ, Burne MJ, Rabb H, Pearse D, Tuder
607 RM, Garcia JG. Protective effects of sphingosine 1-phosphate in murine endotoxin-
608 induced inflammatory lung injury. *Am.J.Respir.Crit Care Med.*2004 **169**, 1245-1251.

609 Potente M, Gerhardt H, Carmeliet P. Basic and therapeutic aspects of angiogenesis.
610 *Cell*2011 **146**, 873-887.

611 Redmer DA, Doraiswamy V, Bortnem BJ, Fisher K, Jablonka-Shariff A, Grazul-Bilska
612 AT, Reynolds LP. Evidence for a role of capillary pericytes in vascular growth of the
613 developing ovine corpus luteum. *Biol Reprod.*2001 **65**, 879-889.

614 Reynolds LP, Grazul-Bilska AT, Redmer DA. Angiogenesis in the corpus luteum.
615 *Endocrine.*2000 **12**, 1-9.

616 Risau W. Mechanisms of angiogenesis. *Nature*1997 **386**, 671-674.

617 Rizk B, Aboulghar M. Modern management of ovarian hyperstimulation syndrome.
618 *Hum.Reprod.*1991 **6**, 1082-1087.

619 Rodewald M, Herr D, Fraser HM, Hack G, Kreienberg R, Wulff C. Regulation of tight
620 junction proteins occludin and claudin 5 in the primate ovary during the ovulatory cycle

621 and after inhibition of vascular endothelial growth factor. *Mol.Hum.Reprod.*2007 **13**,
622 781-789.

623 Roth Z, Hansen PJ. Sphingosine 1-phosphate protects bovine oocytes from heat shock
624 during maturation. *Biol.Reprod.*2004 **71**, 2072-2078.

625 Sanchez T, Estrada-Hernandez T, Paik JH, Wu MT, Venkataraman K, Brinkmann V,
626 Claffey K, Hla T. Phosphorylation and action of the immunomodulator FTY720 inhibits
627 vascular endothelial cell growth factor-induced vascular permeability.
628 *J.Biol.Chem.*2003 **278**, 47281-47290.

629 Schneeberger EE, Lynch RD. The tight junction: a multifunctional complex.
630 *Am.J.Physiol Cell Physiol*2004 **286**, C1213-C1228.

631 Scotti L., Di Pietro M., Pascuali N., Irusta G., de Zúñiga I., Gomez Peña M., Pomilio C,
632 Saravia F., Tesone M., Abramovich D., Parborell F. Sphingosine-1- phosphate restores
633 endothelial barrier integrity in ovarian hyperstimulation syndrome. *Molecular Human*
634 *Reproduction*2016 in press.

635 Scotti L, Abramovich D, Pascuali N, de Z, I, Oubina A, Kopcow L, Lange S, Owen G,
636 Tesone M, Parborell F. Involvement of the ANGPTs/Tie-2 system in ovarian
637 hyperstimulation syndrome (OHSS). *Mol.Cell Endocrinol.*2013 **365**, 223-230.

638 Scotti L, Abramovich D, Pascuali N, Irusta G, Meresman G, Tesone M, Parborell F.
639 Local VEGF inhibition prevents ovarian alterations associated with ovarian
640 hyperstimulation syndrome. *J.Steroid Biochem.Mol.Biol.*2014a **144 Pt B**, 392-401.

641 Scotti L, Abramovich D, Pascuali N, Irusta G, Meresman G, Tesone M, Parborell F.
642 Local VEGF inhibition prevents ovarian alterations associated with ovarian
643 hyperstimulation syndrome. *J.Steroid Biochem.Mol.Biol.*2014b **144 Pt B**, 392-401.

644 Scotti L, Abramovich D, Pascuali N, Irusta G, Meresman G, Tesone M, Parborell F.
645 Local VEGF inhibition prevents ovarian alterations associated with ovarian
646 hyperstimulation syndrome. *J.Steroid Biochem.Mol.Biol.*2014c **144 Pt B**, 392-401.

647 Scotti L, Parborell F, Irusta G, de Z, I, Bisioli C, Pettorossi H, Tesone M, Abramovich
648 D. Platelet-derived growth factor BB and DD and angiopoietin1 are altered in follicular
649 fluid from polycystic ovary syndrome patients. *Mol.Reprod.Dev.*2014d **81**, 748-756.

650 Singleton PA, Dudek SM, Ma SF, Garcia JG. Transactivation of sphingosine 1-
651 phosphate receptors is essential for vascular barrier regulation. Novel role for
652 hyaluronan and CD44 receptor family. *J.Biol.Chem.*2006 **281**, 34381-34393.

653 Spiegel S, Milstien S. Sphingosine-1-phosphate: an enigmatic signalling lipid.
654 *Nat.Rev.Mol.Cell Biol.*2003 **4**, 397-407.

655 Tillet E, Vittet D, Feraud O, Moore R, Kemler R, Huber P. N-cadherin deficiency
656 impairs pericyte recruitment, and not endothelial differentiation or sprouting, in
657 embryonic stem cell-derived angiogenesis. *Exp.Cell Res.*2005 **310**, 392-400.

658 Villasante A, Pacheco A, Ruiz A, Pellicer A, Garcia-Velasco JA. Vascular endothelial
659 cadherin regulates vascular permeability: Implications for ovarian hyperstimulation
660 syndrome. *J.Clin.Endocrinol.Metab*2007 **92**, 314-321.

661 Volk T, Geiger B. A 135-kd membrane protein of intercellular adherens junctions.
662 *EMBO J.*1984 **3**, 2249-2260.

663 Walz A, Keck C, Weber H, Kissel C, Pietrowski D. Effects of luteinizing hormone and
664 human chorionic gonadotropin on corpus luteum cells in a spheroid cell culture system.
665 *Mol.Reprod.Dev.*2005 **72**, 98-104.

666 Wang C, Mao J, Redfield S, Mo Y, Lage JM, Zhou X. Systemic distribution, subcellular
667 localization and differential expression of sphingosine-1-phosphate receptors in benign
668 and malignant human tissues. *Exp.Mol.Pathol.*2014 **97**, 259-265.

669 Woodruff TK, D'Agostino J, Schwartz NB, Mayo KE. Dynamic changes in inhibin
670 messenger RNAs in rat ovarian follicles during the reproductive cycle. *Science*1988
671 **239**, 1296-1299.

672 Xiong Y, Hla T. S1P control of endothelial integrity.
673 *Curr.Top.Microbiol.Immunol.*2014 **378**, 85-105.

674 Yang L, Yatomi Y, Miura Y, Satoh K, Ozaki Y. Metabolism and functional effects of
675 sphingolipids in blood cells. *Br.J.Haematol.*1999 **107**, 282-293.

676 Yatomi Y, Ruan F, Hakomori S, Igarashi Y. Sphingosine-1-phosphate: a platelet-
677 activating sphingolipid released from agonist-stimulated human platelets. *Blood*1995
678 **86**, 193-202.

679

680 **FIGURE LEGENDS**

681 **Figure 1: Effect of S1P treatment on preantral follicles, antral follicles, atretic**
682 **follicles, corpora lutea and cysts from the rat OHSS model.** The graphs show the
683 percentage of each structure in H&E-stained ovarian sections. Different letters indicate
684 significant differences. **(A)** % preantral follicles ($p>0.05$). **(B)** % antral follicles
685 (Control vs OHSS $p<0.05$; OHSS vs OHSS+S1P $p<0.05$). **(C)** % atretic follicles

(p>0.05). **(D)** % corpora lutea (Control vs OHSS p<0.05; OHSS vs OHSS+S1P p<0.01). **(E)** % cysts (Control vs OHSS p<0.001; Control vs OHSS+S1P p<0.01; OHSS vs OHSS+S1P p<0.05). Data are expressed as the mean ± SEM. Results were obtained from three experiments, using 6 rats per group.

Figure 2: Effect of S1P treatment on steroidogenic enzymes levels in ovaries from the rat OHSS model. The levels of proteins in ovarian protein extracts were measured by Western Blotting. The density in each band was normalized to the density of the β-actin or GAPDH band. The lower panels show a representative blot for each protein analyzed. Different letters indicate significant differences. **A)** 3βHSD (Control vs OHSS p<0.05; Control vs OHSS+S1P p<0.05), **B)** P450scc (Control vs OHSS p<0.01; Control vs OHSS+S1P p<0.01) and **C)** StAR (Control vs OHSS p<0.05; OHSS vs OHSS+S1P p<0.05). Data are expressed as the mean ± SEM. Results were obtained from three experiments, using 6 rats per group.

Figure 3: Effect of S1P treatment on ovarian vessels-Corpora lutea from the rat OHSS model. (A) Lectin BS-1 staining in Control, OHSS, and S1P-treated OHSS rats. Graph: Quantification of endothelial cell area in Corpora lutea sections stained in the three groups analyzed. Different letters indicate significant differences (Control vs OHSS p<0.001; OHSS vs OHSS+S1P p<0,001). The photographs show representative histological sections of control, OHSS and OHSS+S1P Corpora lutea stained with lectin BS-1. Scale bars, 100 μm. Three sections per ovary were analysed (six ovaries/group) and at least four corpora lutea were photographed per section. **B)** Immunostaining of periendothelial cells with anti-smooth muscle cell α-actin antibody in control, OHSS, and S1P-treated OHSS rats. Graph: Quantification of periendothelial cell area in Corpora lutea in the three groups analyzed. (Control vs OHSS p<0.001; OHSS vs

OHSS+S1P $p<0.05$; OHSS+S1P vs Control $p<0.01$). The photographs show representative histological sections of control, OHSS, and S1P-treated OHSS rat ovaries stained with anti-smooth muscle cell α-actin antibody. Scale bars, 100 μm. Three sections per ovary were analysed (six ovaries/group) and at least four corpora lutea were photographed per section

Figure 4: Effect of S1P treatment on the expression of adherens and tight junction proteins in ovaries from the rat OHSS model. The graphs show the densitometric analysis for adherens (N-cadherin and VE-cadherin) and tight (claudin-5, occludin, Nectin-2) junction proteins in ovarian protein extracts. **A)** N-cadherin (Control vs OHSS $p<0.05$; OHSS vs OHSS+S1P $p<0.05$), **B)** VE-cadherin (Control vs OHSS $p<0.05$; OHSS vs OHSS+S1P $p<0.01$), **C)** claudin-5 (Control vs OHSS $p<0.01$; OHSS vs OHSS+S1P $p<0.05$) **D)** occludin (Control vs OHSS $p<0.001$; Control vs OHSS+S1P $p<0.05$; OHSS vs OHSS+S1P $p<0.05$) and **E)** Nectin-2 (Control vs OHSS $p<0.05$; Control vs OHSS+S1P $p<0.05$). The density of each band was normalized to the density of the β-actin or GAPDH band. The lower panels show a representative blot for each protein analyzed. Different letters indicate significant differences. Data are expressed as the mean ± SEM. Results were obtained from three experiments, using 6 rats per group.

Figure 5: Effect of S1P treatment on the expression of S1P receptor 1 (S1PR1) in ovaries from the rat OHSS model. Densitometric quantification of S1PR1 levels in ovarian protein extracts. The density of each band was normalized to the density of the GAPDH band. The lower panels show a representative blot for the protein analyzed. Different letters indicate significant differences (Control vs OHSS+S1P $p<0.01$; OHSS

vs OHSS+S1P $p<0.01$). Data are expressed as the mean ± SEM. Results were obtained from three experiments, using 6 rats per group.

Figure 6: Effect of S1P treatment on uterine morphology from the rat OHSS model. H&E stained sections show representative histological fields of Control, OHSS and OHSS+S1P uterus. The dotted lines indicate the thickness of the endometrium. The endometrium from the control group showed a few residual glands with a covering epithelium that is low cuboidal to columnar. On the other hand, the endometrium of the OHSS and S1P-treated OHSS group, showed a tall columnar surface epithelium with pseudostratification and signs of an increased turnover, scattered glands are seen within the thickness of the endometrium. Scale bars, 50 μm. Insets in all panels show images at higher magnification of the endometrial epithelium. Scales bars, 5 μm.

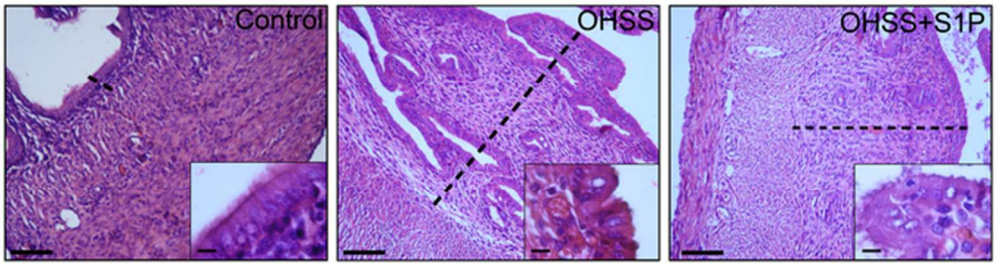

57x18mm (300 x 300 DPI)

Table I: Effect of S1P treatment on ovarian weight and serum progesterone concentration in a rat OHSS model.

	Control (n=6)	OHSS (n=6)	OHSS+S1P (n=6)
Ovarian weight (g)	0.057 ±0.003[a]	0.122±0.004[b]	0.093±0.007[c]
Serum progesterone (ng/ml)	64.01±18.93[a]	173.70±15.31[b]	63.45±18.15[a]

Note: Data are expressed as mean ± SEM; n = 6 rats/group. Letters indicate a significant statistical difference between groups by one-way ANOVA, followed by Tukey's multiple comparison test. Ovarian weight: a vs b $P<0.001$; a vs c $P<0.01$; b vs c $P<0.05$. Serum progesterone: a vs b $P < 0.001$